Advanced Fiber Materials (2022) 4:43–65
https://doi.org/10.1007/s42765-021-00088-6

REVIEW

Electrospinning Engineering Enables High-Performance Sodium-Ion Batteries

Chuanping Li[1] · Min Qiu[2] · Ruiling Li[1] · Xuan Li[1] · Manxi Wang[1] · Jiabo He[1] · Ganggang Lin[3] · Liren Xiao[2] · Qingrong Qian[1] · Qinghua Chen[1] · Junxiong Wu[4] · Xiaoyan Li[1] · Yiu-Wing Mai[5] · Yuming Chen[1]

Received: 18 March 2021 / Accepted: 1 May 2021 / Published online: 7 July 2021

Abstract

As a promising energy storage device, sodium-ion batteries (SIBs) have received continuous attention due to their low-cost and environmental friendliness. However, the sluggish kinetics of Na ion usually makes SIBs hard to realize desirable electrochemical performance when compared to lithium-ion batteries (LIBs). The key to addressing this issue is to build up nanostructured materials which enable fast Na-ion insertion/extraction. One-dimensional (1D) nanocarbons have been considered as both the anode and the matrix to support active materials for SIB electrodes owing to their high electronic conductivity and excellent mechanical property. Because of their large surface areas and short ion/electron diffusion path, the synthesized electrodes can show good rate performance and cyclic stability during the charge/discharge processes. Electrospinning is a simple synthetic technology, featuring inexpensiveness, easy operation and scalable production, and has been largely used to fabricate 1D nanostructured composites. In this review, we first give a simple description of the electrospinning principle and its capability to construct desired nanostructures with different compositions. Then, we discuss recent developments of carbon-based hybrids with desired structural and compositional characteristics as the electrodes by electrospinning engineering for SIBs. Finally, we identify future research directions to realize more breakthroughs on electrospun electrodes for SIBs.

Keywords Sodium-ion batteries · Electrospinning engineering · Carbonaceous substrate · Hybrid

Introduction

With the decrease of fossil fuels, energy crisis and environmental pollution have become increasingly serious. The development and utilization of renewable energy play a critical role in solving these problems. However, renewable energy is often intermittent due to the influence of weather, region, climate and other conditions. Therefore, energy storage devices must be developed to make sustainable and universal use of renewable energy [1, 2]. Due to their high energy density and long cycle life, lithium-ion batteries (LIBs) are popular and have been widely used in portable electronic devices and electric vehicles. Even though the development of LIBs prevails, their disadvantages must be taken into account. The lithium resource is not abundant and its geographic distribution is uneven [3, 4]. It is hence imperative to develop other low-cost and high-performance batteries. Sodium-ion batteries (SIBs) with similar energy storage mechanisms to LIBs have been regarded as a promising alternative due to the natural abundance and low cost of sodium [5, 6].

Chuanping Li and Min Qiu contributed equally.

✉ Junxiong Wu
jwuba@connect.ust.hk

✉ Xiaoyan Li
xiaoyanli1985@126.com

✉ Yiu-Wing Mai
yiu-wing.mai@sydney.edu.au

✉ Yuming Chen
yumingc126@126.com

1 College of Environmental Science and Engineering, Fujian Normal University, Fuzhou 350000, Fujian, China

2 College of Chemistry and Materials Science, Fujian Normal University, Fuzhou 350000, China

3 State Grid Fujian Maintenance Company, Fuzhou 350000, Fujian, China

4 Department of Mechanical Engineering, The Hong Kong Polytechnic University, Kowloon, Hong Kong, China

5 Centre for Advanced Materials Technology (CAMT), School of Aerospace, Mechanical and Mechatronics Engineering J07, The University of Sydney, Sydney, NSW 2006, Australia

However, the large radius of sodium ions (1.02 Å for Na^+ versus 0.76 Å for Li^+) leads to sluggish kinetics in the electrodes, giving rise to the poor electrochemical performance of SIBs [7]. At this time, it is necessary to find carrier materials that are sufficient to allow large ions, such as sodium ions, to shuttle freely. One-dimensional (1D) nanostructures are attractive because they have abundant active sites and high deformation stress that can enhance the reaction kinetics of the electrodes [8, 9]. There are many techniques to prepare 1D nanostructures, including self-assembly, chemical vapor deposition (CVD), electrospinning, polymerization, hydrothermal, and template methods [10, 11]. Among these methods, electrospinning technology is simple, effective, low-cost with great potential to tune the structural and compositional features. Moreover, 1D nanomaterials can also be assembled into two-dimensional (2D)/three-dimensional (3D) architectures by electrospinning, which benefits ion diffusion and electrode structural integrity [12–15]. Recently, electrospinning technology has been widely used in the process of preparing electrode materials for sodium-ion batteries. A simple electrospinning method is used to prepare high-performance nano-materials to construct an efficient electrode structure for SIBs including, for example, amorphous $NiMoO_4$/graphene dendritic nanofibers [16], carbon-nanochain concatenated hollow Sn_4P_3 nanospheres architectures [17], nitrogen (N) doped carbon nanofibers sheathed SnSe quantum-dots [18], FeS_2 nanoparticles embedded in N/S co-doped porous carbon fibers [19], carbon-encapsulated CoS_2 nanoparticles anchored on N-doped carbon nanofibers [20], 3D hierarchical Sn/NS-CNFs@rGO network [21], red phosphorus/carbon nanofibers/graphene free-standing paper anode [22], graphene highly scattered in porous carbon nanofibers [23] and electrospun $Na_3V_2(PO_4)_3$/C nanofibers [24]. These excellent and novel materials can be used as self-supporting anodes and cathodes for SIBs. They provide a smooth transmission channel for Na^+, accelerate long-distance electron transfer, ensure fast reaction kinetics, and alleviate volume expansion. In addition, a modified cellulose acetate separator (MCA) for SIBs has been synthesized through the electrospinning process, and the interface chemical group was optimized by partially replacing the acetyl group with the hydroxyl group. The flexible MCA separator displays good chemical stability and wettability in electrolytes (contact angle is close to 0°) [25]. To prepare high-performance SIBs through electrospinning technology, some problems have to be resolved. First, we need to optimize the electrospinning parameters. Thus, the needle will be blocked if the viscosity of the precursor solution is too high, whereas dripping occurs if a dilute solution is used. As a result, the fiber diameter is not uniform, reducing the application value of the material. In addition, it is necessary to consider the regulation of voltage and current to ensure that it works under a stable voltage and current. Second, "hybrids" are a simple and practical way to improve the materials. The above issues indicate that both experimental attempts and fundamental understanding of electrospinning are required.

In this review, we first give a simple description of the electrospinning principle and its ability to construct the desired nanostructures with different compositions. Then, we summarize the latest developments on electrospinning technology to use carbon-based hybrid materials with required structure and composition characteristics as electrodes for SIBs. Finally, we discuss future research directions to achieve new breakthroughs in electrospun SIB electrodes.

Electrospinning

Principle of Electrospinning

The electrospinning technique has been invented since 1934. It is an effective and simple technology to synthesize 1D nanofibrous materials with well-controlled diameters (10^1–10^3 nm) [26, 27]. The electrospinning unit principally consists of three parts: a high-voltage power supply, a metallic needle nozzle, and a collector [28–30]. In a typical electrospinning process, when a high voltage is applied between a collector and a needle at a suitable distance, the small droplets of the electrically conductive polymer solution can be stretched to a "Taylor cone". The charged droplets will be ejected from the needle tip when the electrostatic force surpasses the surface tension of the liquid. The charged liquid experiences an intricate bending, elongating, and whipping motion. Meanwhile, the flow becomes thinner with quick solvent evaporation and solid nanofibers are eventually gathered on the collector (Fig. 1) [29, 31]. Polymer nanofibers can be produced via electrospinning by dissolving the precursors in suitable solvents, for example, polyacrylonitrile (PAN) and polyvinylpyrrolidone (PVP) dissolved in dimethylformamide (DMF) [32, 33]. The diameter of the nanofibers achieved by electrospinning is affected by many factors, which include the viscosity, concentration, molecular weight and surface tension of the precursor solution, electrical conductivity, as well as the voltage and environmental temperature and humidity. High viscosity (concentration) normally leads to the formation of nanofibers with a large diameter, while low viscosity of the solution is beneficial for preparing nanofibers with a small diameter. Uniform nanofibers can be obtained at high voltage, but an excessively high voltage will result in the formation of beads. In addition, it tends to form nanofibers with reduced diameters at a large distance between nozzle and collector. The environment is a key factor affecting the solvent evaporation process. High temperature accelerates the evaporation of solvents, resulting in the formation of nanofibers with decreasing diameter.

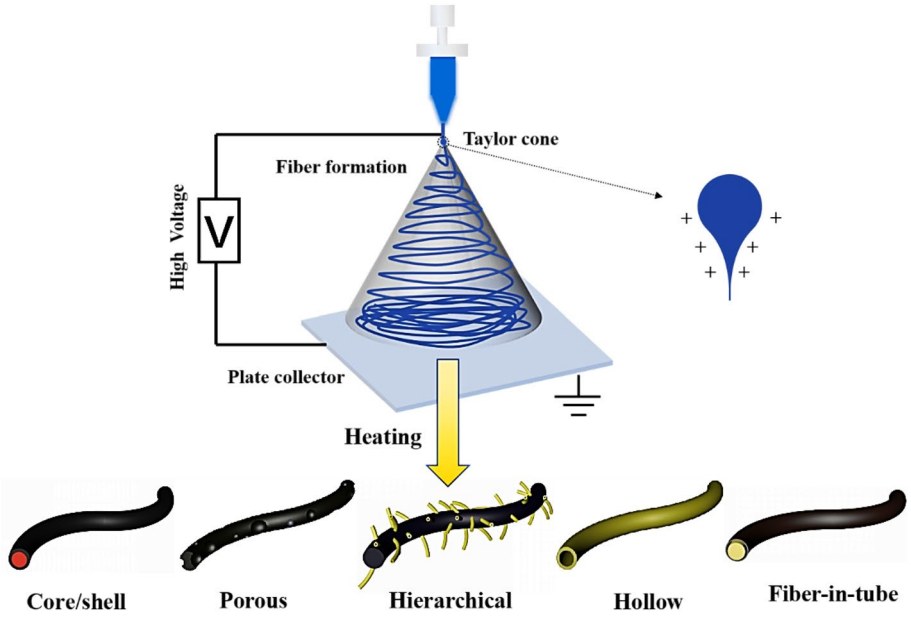

Fig. 1 Schematic illustrations of structural design through electrospinning engineering

Therefore, if these parameters can be reasonably optimized, the diameter of nanofibers can be well-controlled [34–36]. The versatility of electrospinning enables the fabrication of nanomaterials with different advanced architectures [37]. To tune the structural and compositional features of the electrospun nanofiber, post-treatments including heat treatment, hydro-thermal method, and activation process are of great importance. The electrospun materials can be converted into carbon, metal oxide and their hybrids through high-temperature treatment at a special atmosphere including N_2, Ar, Ar/H_2 and O_2. A porous structure is usually produced during this process due to the removal of the template and the formation of gases. For example, phosphorus-doped porous carbon nanofibers (CNFs) were obtained by calcination of PAN/polyethylene glycol (PEG)/polyphosphoric acid (PPA) composite nanofibers in N_2 [38, 39]. Electrospinning technology is a low-cost and powerful technique that can produce diverse nanomaterials on a large scale. Section 3 gives a detailed discussion on how electrospinning has been used to construct advanced anodes and cathodes for SIBs.

Structural Design Through Electrospinning

Over the past decade, substantial interest has been focused on the exploration of new electrode materials with various architectures because their electrochemical performance is closely related to the structures. For example, nanoscale engineering can significantly reduce the ion diffusion length and accommodate the internal strain, thus resulting in improved cyclic stability and rate performance. Also, a porous structure provides a convenient way for the effective transport and diffusion of the electrolytes and ions. The design of porous and/or hollow structures can alleviate the structural strain and buffer volume changes of the electrode materials during the repeated charge/discharge processes, contributing to excellent cyclic stability. Hence, the rational design of electrode materials with various structures and morphologies is critical to their electrochemical performance. Below we will summarize various nanostructures and morphologies of the nanomaterials through electrospinning engineering.

Core/Shell Structure

Coaxial electrospinning is one of the most common methods used to prepare intriguing core/shell structures (Fig. 1) [40]. The key to obtaining the core/shell structure is the immiscibility between the core and shell solutions. For example, the core/shell oil@phosphomolybdic acid (PMOA)/PAN composite nanofibers can be synthesized by using mineral oil as the core solution and the mixture of PMOA and PAN dissolved in the DMF as the shell solution [37]. Further, single-needle electrospinning combined with post-treatment can enable the core/shell structure. For example, when ammonium molybdate tetrahydrate (AMM)/polyvinyl alcohol (PVA) composite nano-fibers were prepared by single-needle electrospinning, the core/shell MoO_2@carbon nanofibers can be produced after a simple anneal process. With increasing ratio of AMM in PVA/AMM mixture, a part of AMM nanoparticles cannot be embedded in the center of the hybrid nanofibers. After annealling, MoO_3 can be reduced to MoO_2 by carbon from the decomposition of PVA

and MoO_2 accumulates in the center of the hybrid nanofibers [41]. The core/shell structure can also be produced by coating another layer with different composition on the prepared nanofibers through in situ redox deposition.

Porous Structure

Porous structure can be made by selectively removing the sacrificial materials, which has been considered as a most efficient method. The sacrificial components include organic, inorganic and organic/inorganic materials, which can be removed by heat and solution treatments (Fig. 1). In a recent study, Shan et al. first prepared ZIF-8/PAN composite nanofibers. During the heating process, ZIF-8 decomposed and generated Zn nanoparticles, which were then removed by HCl leaching, thus forming porous carbon nanofibers [42].

Hierarchical Structure

Hierarchical structures comprise nanotubes, nanoparticles and nanosheets, etc. Electro-spinning combined with post-treatment can give hierarchical structures. In general, different methods/processes are made to integrate various functional precursors that are converted into different compositions and structures, yielding a unique hierarchical structure. For example, Li et al. developed a CVD system using in situ formed C_2H_2 from the decomposition of the sacrificial polymer as the carbon source and nickel from the reduction of nickel acetate as the catalyst. Consequently, carbon nanotubes (CNTs) were generated on the electrospun CNFs to yield CNT/CNF hybrids (Fig. 1). With these structural features, the hybrids displayed excellent performance for LIBs [43].

Hollow Structure

The hollow structure has attracted increasing interest because of its unique properties, such as high specific surface area [44–46]. Coaxial electrospinning technique is a simple and effective approach to synthesize hollow tubular structures, whereby the core serves as the template. Oil and polymers that can be easily removed are widely used as the core, which can be decomposed after calcination or dissolved in a suitable solvent. Also, the shell is converted into the designed materials after annealing, hence forming hollow nanofibers. Additionally, constructing a bicomponent core is another way to create the hollow structure as long as these two components can react to form gas and others which can be evaporated. For example, Chen et al. [47] made a core/shell structure with a ZnO_x/carbon core. During the heating process, ZnO_x etched the carbon forming CO_x and Zn, and then Zn was evaporated at high temperature, creating hollow carbon nanofibers [47].

Fiber-in-Tube Structure

Although hollow structure greatly shortens the transport path and effectively buffers the volume changes of electrode materials during the Na insertion and extraction process, one major issue associated with the hollow structure is its low tap density, thus sacrificing the energy density of batteries. For comparison, the fiber-in-tube design not only maintains the merits of hollow structure but also has a higher tap density, making it a more advanced architecture. The method to synthesize the fiber-in-tube structure is more difficult and complicated compared to the hollow structure. The control of interface separation of core–shell structure is the key to the synthesis of such architecture. During the reaction process, the outer layer and inner layer suffer from different volume changes and then enable the interface separation of the core–shell structure, producing a gap between the outer layer and inner layer. For example, Li et al. [48] grew a ZIF-67 layer onto the electrospun PAN/ZIF-67 composite nanofibers. During the sulfuration process, the fiber-in-tube structure can be formed due to the diffusion-controlled reaction mechanism. After the calcination treatment, Co_9S_8–carbon/Co_9S_8 hybrid with fiber-in-tube structure is obtained (Fig. 1).

Sodium-Ion Batteries

Cathodes

The cathode materials in the SIBs are responsible for providing active sodium ions to complete the charging and discharging processes, which are crucial to high energy density. Therefore, the development and modification of the cathode materials for Na-storage are the hot spots. The exploitation of cathode materials for SIBs should meet the following requirements [49]: (i) high specific capacity, (ii) high redox potential, (iii) stable structure with little phase transformation during the Na^+ intercalation/deintercalation processes, (iv) high sodium-ionic and electronic conductivity, and (v) abundant resources, nontoxicity and low-cost. However, due to the large radius and molecular mass of Na^+, the kinetics of Na^+ is sluggish. The stability of the cathode materials is also affected when Na^+ is inserted. It has been proven that the performance of cathode materials can be significantly improved by electrospinning [50]. The research on the preparation of cathode materials for SIBs by electrospinning technology

has developed rapidly. Generally, cathode materials with benign Na-storage capacity and stable structure can be classified into two major groups: polyanion compounds and transition metal oxides [28].

Hybrid Cathodes Based on Carbon and Polyanionic Compounds

Polyanionic compounds are one of the most attractive cathode materials for SIBs in view of their stable framework structure, which ensures a good cycle life [50]. In addition, some polyanionic groups show a strong promoting effect, which has a great influence on the battery voltage. However, this material is hampered by low electronic conductivity and sluggish kinetics. Numerous strategies have emerged to address the abovementioned problems. Electrospinning is a promising process to control the morphology/structure of the cathode materials and the decoration (coating layer) of conductive materials, such as CNTs, CNFs and graphene [51].

Orthophosphate Cathode Materials Polyanionic orthophosphate cathode materials endow excellent safety and cycling performance in SIBs owing to their stable structure. Although their specific capacity is low, yet they are still potential candidates for cathode materials. Previous studies mainly focused on surface coating, element doping, and substitution to improve their electrochemical performance [52]. $Na_3V_2(PO_4)_3$ (NVP) is a typical NASICON structural material with a convenient and efficient sodium-ion transport path [50]. In 2014, Liu et al. [53] embedded NVP particles within porous CNFs (diameter: ~ 20–30 nm) through electrospinning (Fig. 2a). Reversible capacities of 101 and 39 mAh g^{-1} were maintained at 0.1 and 10 C (1C = 117 mAh g^{-1}), respectively. In the same year, Kajiyama et al. [54] successfully fabricated NVP cathodes with a core–shell structure via electrospinning, where NVP nanoparticles are encapsulated in CNFs. The high reversible capacity of 94 mAh g^{-1} at 1 C was obtained with a capacity retention rate of 74% after 50 cycles. Li et al. [55] proved that the electrochemical performance of the NVP/C(carbon) nanorods through the electrospinning technology had significantly improved. The initial discharge capacity was up to 116.9 mAh g^{-1} and 105.3 mAh g^{-1} at the rates of 0.05 and 0.5 C, respectively, and the capacity was still maintained 97.5 mAh g^{-1} after 50 cycles at 0.5 C. Li et al. [56] also prepared special budding-willow-branches NVP/C nanofibers with uniform distribution of outer carbon layer around the inner NVP layer to form willow branches (Fig. 2b). This structure effectively improved the electrical conductivity and exhibited an exceptional rate capability of 106.8 mAh g^{-1} and 103 mAh g^{-1} at 0.2 and 2 C, respectively. The cycle performance is superior (107.2 mAh g^{-1} after 125 cycles). Subsequently, Yang et al. [57] prepared hierarchical NVP/C nanofibers that could effectively accelerate the transfer of Na^+/electron. The synthesized nanofiber manifested the superior rate capability of 76.9 mAh g^{-1} at a high current density of 100 C, and the specific capacity remained at 112 mAh g^{-1} after 250 cycles at 1 C, suggesting excellent cycling stability. Furthermore, Ni et al. [58] made 3D electronic fibrous channels wrapping with NVP particles (0.1–1 μm) as a flexible electrode. The prepared cathodes exhibited a remarkable rate capability of 116 and 71 mAh g^{-1} at 0.1 and 20 C, respectively, and the capacity retention was 88.6% after 150 cycles at 0.5 C. Besides $Na_3V_2(PO_4)_3$, $NaTi_2(PO_4)_3$ is another promising NASICON material with a theoretical specific capacity of 133 mAh g^{-1}. However, its cycle life and rate capability still need to be improved. Li et al. [59] prepared $NaTi_2(PO_4)_3$/C nanofibers through electrospinning, which delivered reversible capacities of 87 and 63 mAh g^{-1} at 10 and 20 C, respectively, much better than those of carbon-free $NaTi_2(PO_4)_3$ fibers and $NaTi_2(PO_4)_3$ nanoparticles (Fig. 2b). Besides, Yu et al. [60] synthesized $NaTi_2(PO_4)_3$ embedded in 1D N-doped CNFs. The fabricated cathode displayed outstanding rate and cycling performance (a specific capacity of 105 mAh g^{-1} remained after 20,000 cycles at 10 C) due to high electronic conductivity. Dong et al. [61] prepared $Na_2VTi(PO_4)_3$/C nanofibers with a crosslinked structure as a flexible electrode by combining electrospinning and calcination. The assembled full cell exhibited a plateau of ~ 1.2 V with a capacity retention rate of 83% after 600 cycles at alternating rates of 4 C (Fig. 2c).

$NaFePO_4$ has been widely investigated because of the successful application of $LiFePO_4$ cathode in LIBs. The crystal structure of $NaFePO_4$ is mainly divided into two types, olivine (o-$NaFePO_4$) and maricite (m-$NaFePO_4$) [62]. Akin to $LiFePO_4$, o-$NaFePO_4$ shows high electrochemical activity but a labile structure. Although phase change does not easily occur in m-$NaFePO_4$, the Na^+ diffusion channels can be blocked, leading to electrochemical inactivity [28]. Moreover, it is easier to prepare m-$NaFePO_4$ when compared to o-$NaFePO_4$. Kim et al. [62] prepared nanostructured m-$NaFePO_4$ coated with carbon, thus successfully enabling Na^+ to leave the structure freely. The electrode showed a specific capacity of 142 mAh g^{-1} at 0.05 C for the first discharge cycle, with a capacity retention rate of 95% after 200 cycles. Liu et al. [63] recently designed an ingenious technique combining electrospinning to fabricate $NaFePO_4$ nanodots (with only 1.6 nm diameter) embedded within the porous N-doped CNFs (Fig. 2d). The reversible capacities were 145 and 61 mAh g^{-1} at 0.2 and 50 C (1C = 150 mAh g^{-1}), respectively. The prepared electrode possessed prominent long cycle life up to 6300 cycles.

Fluorophosphate Cathode Materials Fluorophosphate, such as $NaVPO_4F$ and Na_2MPO_4F (M = Fe, Mn, Co), is one kind of high-voltage cathode materials due to the strong induc-

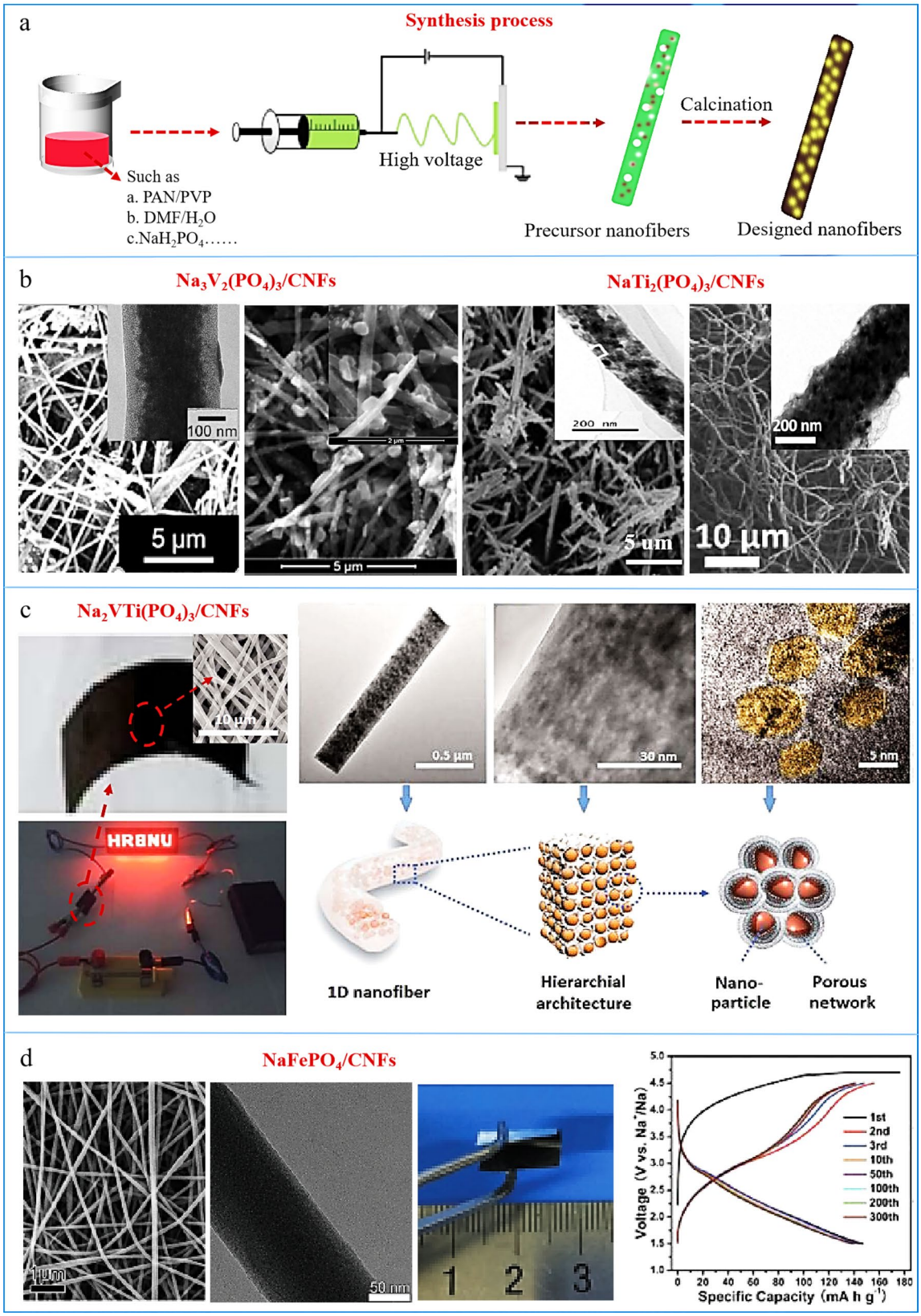
a
Synthesis process
Such as
a. PAN/PVP
b. DMF/H_2O
c.NaH_2PO_4……
High voltage
Calcination
Precursor nanofibers
Designed nanofibers
b
$Na_3V_2(PO_4)_3$/CNFs
$NaTi_2(PO_4)_3$/CNFs
100 nm
5 μm
5 μm
200 nm
5 um
200 nm
10 μm
c
$Na_2VTi(PO_4)_3$/CNFs
HRBNU
0.5 μm
30 nm
5 nm
1D nanofiber
Hierarchial architecture
Nano-particle
Porous network
d
$NaFePO_4$/CNFs
1 μm
50 nm
1 2 3
Voltage (V vs. Na^+/Na)
Specific Capacity (mA h g^{-1})
1st
2nd
3rd
10th
50th
100th
200th
300th

◂**Fig. 2** Synthesis of electrospun orthophosphate cathode material. **a** Schematic illustration for the preparation process and image illustration of orthophosphate cathode material. **b** Image illustration of $Na_3V_2(PO_4)_3$/CNFs and $NaTi_2(PO_4)_3$/NCNFs. Reproduced with permission [54]. Copyright 2014, Wiley–VCH. Reproduced with permission [56]. Copyright 2015, Elsevier. Reproduced with permission [59]. Copyright 2017, Elsevier. Reproduced with permission [60]. Copyright 2018, Frontiers S.A. **c** Photographs, SEM image and application of $Na_2VTi(PO_4)_3$/CNFs, image illustration and schematic of hierarchical structure of the hybrid nanofiber. Reproduced with permission [61]. Copyright 2017, Royal Society of Chemistry. **d** SEM image and photographs of $NaFePO_4$/CNFs, galvanostatic charge/discharge profiles at a current density of 20 mA g^{-1}. Reproduced with permission [63]. Copyright 2018, Wiley–VCH

tion effect of F^-. Barker, Saidi and Swoyer [64] showed that the initial discharge capacity of synthesized $NaVPO_4F$ was only 82 mAh g^{-1}, with less than 50% capacity left after 30 cycles. To improve the potential applications of $NaVPO_4F$, Jin et al. [65] used the electrospinning technique to fabricate 1D porous $NaVPO_4F$/C nanofibers, where the $NaVPO_4F$ nanoparticles were encapsulated inside the 3D conductive carbon network, effectively promoting the Na^+/electrons transmission, thereby realizing a high reversible capacity of 103 mAh g^{-1} at 143 mA g^{-1} and a superior cycling performance (capacity retention of 96.5% after 1000 cycles) (Fig. 3a). Hu et al. [66] successfully designed 3D conductive CNFs uniformly encapsulated with Na_2MnPO_4F nanoparticles (10–30 nm), which helped transport Na^+/electrons. The prepared electrode showed an initial discharge capacity as high as 122.4 mAh g^{-1} at 6.2 mA g^{-1} and a distinct voltage platform of 3.6 V. Wang et al. [67] also embedded Na_2FePO_4F nanoparticles (~3.8 nm) in porous CNFs by electrospinning. The reversible capacity was 117.8 mAh g^{-1} at 0.1 C (1C = 124 mA g^{-1}), and a capacity of 46.4 mAh g^{-1} was retained even at a higher current density of 20 C. The prepared electrode also displayed a long cycle life with 85% capacity retention after 2000 cycles.

Pyrophosphate Cathode Materials Pyrophosphates are an important branch of phosphate cathode materials. Their synthesis process is relatively simple, and the strong P-O bond in the crystal structure provides a stable framework for pyrophosphates, which is beneficial for Na^+ transport [50]. Niu et al. [68] first studied the theoretical capacity of $Na_{6.24}Fe_{4.88}(P_2O_7)_4$ reaching 117.4 mAh g^{-1}. Then they [69] successfully used graphene to wrap $Na_{6.24}Fe_{4.88}(P_2O_7)_4$ (NFPO) by electrospinning to form NFPO/C/rGO (Fig. 3b). The prepared NFPO/C/rGO cathode displayed a discharge capacity of 99 mAh g^{-1} after 320 cycles at 40 mA g^{-1}, and a discharge capacity of 53.9 mAh g^{-1} at a higher current density of 1280 mA g^{-1}, which was 1.6 times higher than that of the NFPO/C composite.

Sulfate Cathode Materials The properties of sulfate materials, including $NaFeSO_4F$ and $Na_{2+2x}M_{2-x}(SO_4)_3$ (M = Fe, Mn), are somewhat similar to fluorophosphate, with the strong electronegativities of $(SO_4)^{2-}$ resulting in higher energy densities and operating potentials. Fe-sulfate is most popular because of its low price and superior performance [70]. Meng et al. [70] synthesized $Na_{2+2x}Fe_{2-x}(SO_4)_3$ composite modified with monolayer CNT, showing superior rate capability and cycling performance. Yu et al. [71] synthesized porous graphite carbon nanofiber (PCNF) film incorporated with $Na_{2+2x}Fe_{2-x}(SO_4)_3$ nanoparticles using a simple electrospinning technique combined with electro-spraying (Fig. 3c). After 500 cycles at 5 C and 40 C, the capacity retention exceeded 95%, confirming that the porous flexible structure with scalability enabled the hybrid membrane to achieve high specific capacity and long cycle life.

Anodes

Carbonaceous Anodes

Carbonaceous materials are widely studied as anodes for SIBs because of their stable structure, good electronic conductivity, and easy preparation [72–77]. Many carbonaceous materials can be used as SIB anodes, such as CNFs, carbon hollow tubes (CHTs), graphene nanosheets, CNF/graphene hybrids, and heteroatom-doped hybrids.

CNFs 1D CNFs have received extensive attention as SIB anodes due to their excellent electronic/ionic conductivity and unique structure [78]. Bai et al. [79] reported electrospun polyvinyl chloride (PVC)-derived CNFs with excellent cycle stability and rate performance. Chen et al. [80] obtained uniform CNFs using PAN as the raw material through electrospinning and subsequent heat treatment, displaying reversible capacities of 233 and 82 mAh g^{-1} at 50 and 2000 mA g^{-1}, respectively. Also, the capacity retention rate of 97.7% can be reached after more than 200 cycles. Jin, Shi and Wang [81] systematically investigated the effect of carbonization temperature (800–1500 °C) on the electrochemical performance of PAN-derived CNFs and pointed out that different carbonization temperatures would lead to different degrees of graphitization, microstructures, and sodium storage capacities. In their work, CNFs obtained at 1250 °C delivered a maximum capacity of 275 mAh g^{-1} at 20 mA g^{-1}. To reduce the contact resistance, Guo et al. [82] designed binder-free CNF films with $Cu(NO_3)_2$ as the crosslinking agent. The specific capacity of the crosslinked CNFs film was 449 mAh g^{-1} at 50 mA g^{-1}. The capacities of 126 and 111 mAh g^{-1} were maintained after 500 cycles at 5 and 10 A g^{-1}, respectively, with no degradation of capac-

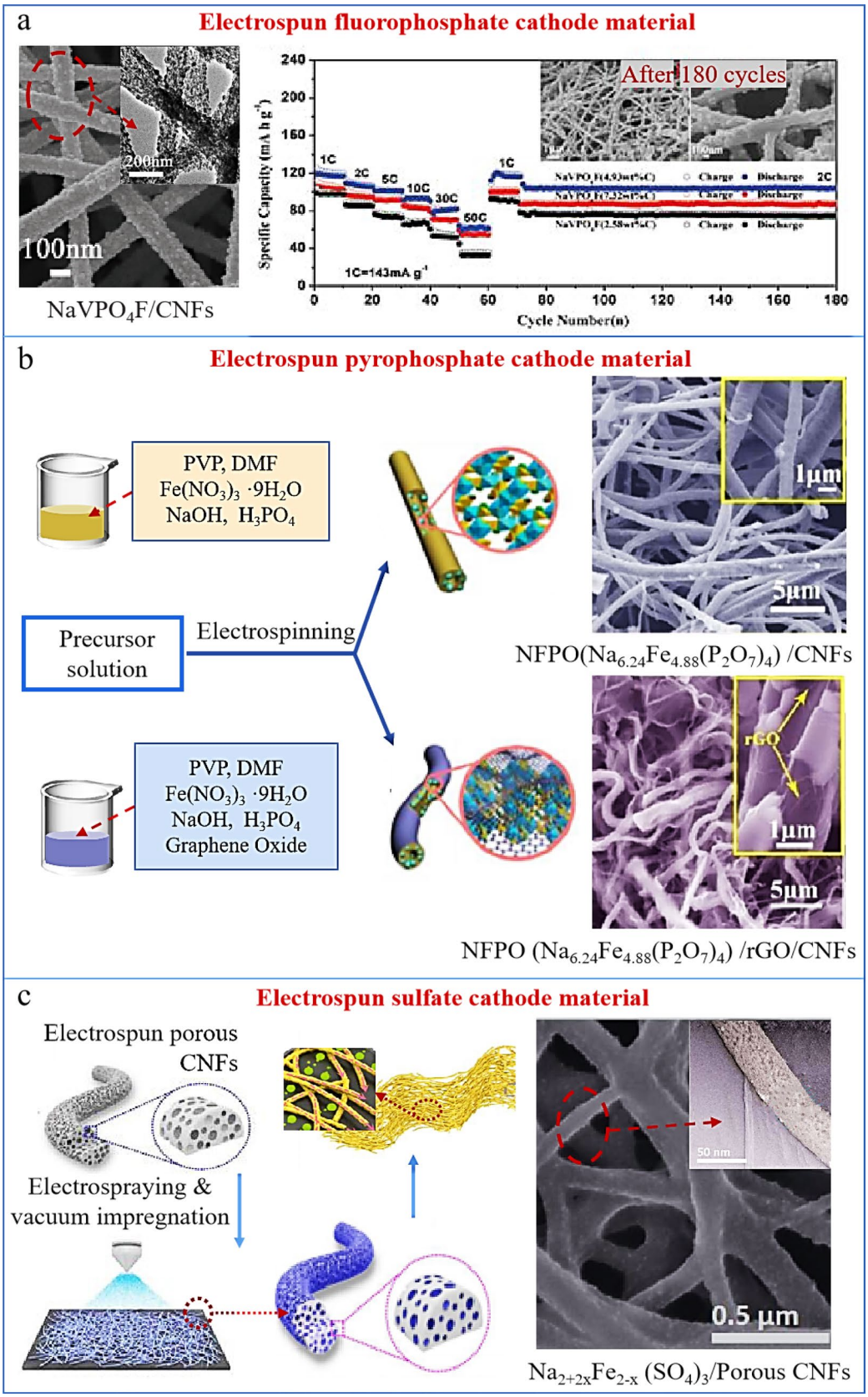
a
Electrospun fluorophosphate cathode material
200nm
100nm
NaVPO4F/CNFs
After 180 cycles
Specific Capacity (mA h g-1)
Cycle Number(n)
1C=143mA g-1
1C
2C
5C
10C
30C
50C
Charge
Discharge
b
Electrospun pyrophosphate cathode material
PVP, DMF
Fe(NO3)3 ·9H2O
NaOH, H3PO4
Precursor solution
Electrospinning
1μm
5μm
NFPO(Na6.24Fe4.88(P2O7)4) /CNFs
PVP, DMF
Fe(NO3)3 ·9H2O
NaOH, H3PO4
Graphene Oxide
rGO
1μm
5μm
NFPO (Na6.24Fe4.88(P2O7)4) /rGO/CNFs
c
Electrospun sulfate cathode material
Electrospun porous CNFs
Electrospraying & vacuum impregnation
50 nm
0.5 μm
Na2+2xFe2-x (SO4)3/Porous CNFs

◂**Fig. 3** Synthesis of electrospun fluorophosphate/pyrophosphate/sulfate cathode materials. **a** Image illustration of $NaVPO_4F$/CNFs, rate capability of $NaVPO_4F$/C with different carbon content (inset: SEM images of $NaVPO_4F$/C with different magnification after 180 cycles). Reproduced with permission [65]. Copyright 2017, Wiley–VCH. **b** Schematic of the synthetic process and SEM image of NFPO/C and NFPO/rGO/C composites. Reproduced with permission [69]. Copyright 2017, Royal Society of Chemistry. **c** Schematic illustration for the preparation process and image illustration of $Na_{2+2x}Fe_{2-x}(SO_4)_3$/porous CNFs hybrid film. Reproduced with permission [71]. Copyright 2016, Royal Society of Chemistry

ity. The excellent electrochemical performance could be attributed to the special crosslinked structure, which enabled fast ion diffusion and electron transfer kinetics, and a robust structure to withstand the repeated internal stresses originated from the repeated insertions and extractions of Na^+ during cycling.

Porous/Hollow Carbon Porous carbon is usually composed of randomly distributed graphitized micro-domains, twisted graphene nanosheets and voids. This unique structure with randomly distributed and crosslinked graphite micro-domains tends to maintain an amorphous structure and inhibit the conversion to a graphite structure. Maier [83] emphasized that particle size and morphology had crucial influences on mass transfer, so the electrochemical performance can be optimized by structure design. Therefore, porous CNFs with high specific surface areas can be a good candidate to store Na^+. Wang et al. [84] used the triblock copolymer F127 as a soft template to prepare flexible porous CNFs (P-CNFs), displaying a reversible capacity of 266 mAh g^{-1} at 0.2 C after 100 cycles. This excellent performance was directly caused by the stable 3D porous conductive network structure. In addition, Wang et al. [85] synthesized a flexible porous N-doped CNF membrane by electrospinning, delivering reversible capacities of 377 and 154 mAh g^{-1} at 100 and 15,000 mA g^{-1}, respectively. Notably, the capacity of 210 mAh g^{-1} at 5000 mA g^{-1} remained after 7000 cycles. Dirican and Zhang [86] prepared porous carbon microfibers (PCMFs) by electrospinning. The resultant PCMF electrode, as an anode for SIBs, showed a reversible capacity of 242 mAh g^{-1} after 200 cycles (89% capacity retention rate) (Fig. 4a). Further, the introduction of hollow structure into porous carbons can further enhance the contact surface areas, which will facilitate the transport of ions and electrons, hence yielding excellent electrochemical performance. Chen et al. [47] used the self-etching and graphitization methods to synthesize porous carbon hollow nanotubules (CHTs) (Fig. 4a). The prepared porous CHTs had a 1D tubular morphology with a length of several microns and a diameter of 170–200 nm. The hollow tubular structure and rough surface promoted the effective transport of ions. Benefiting from advanced structure design, porous CHTs delivered a high capacity up to 346 mAh g^{-1}, good rate capability of 128 mAh g^{-1} at 7 A g^{-1}, and excellent cycling performance of ~ 140 mAh g^{-1} at 4.5 A g^{-1} after 10,000 cycles.

Heteroatom-Doped Carbon Heteroatom doping will increase the actives sites and the electronic/ionic conductivity [87–91]. Among various heteroatoms, the doping of N and sulfur (S) has been extensively studied [92–96]. N doping can contribute more electrons to the π-conjugated system of carbon, thereby increasing the electronic conductivity of CNFs [97, 98]. In addition, pyridine-N and pyrrole-N carbon can produce defects in CNFs, providing more diffusion channels and active sites for Na^+ insertion [99]. Zhu et al. [88] synthesized electrospun N-doped CNFs with a high reversible capacity of 293 mAh g^{-1} at 50 mA g^{-1}. Chen et al. [100] produced N-doped CNFs with urea as the nitrogen source. It was found that the N-doped CNFs with high nitrogen content (19.06%) showed a high reversible capacity of 354 mAh g^{-1} at 50 mA g^{-1}. The capacity of 201.5 mAh g^{-1} was still maintained after 1000 cycles with a 93.29% retention rate. Wang et al. [85] used polyamic acid as the polymer precursor to prepare electrospun N-doped CNFs. These fabricated flexible N-doped CNFs showed a 3D nano-porous network, a high amount of nitrogen doping, high structural durability and excellent mechanical flexibility. This unique nanostructure effectively promoted the insertion and extraction of Na^+, enabling a high reversible capacity of 210 mAh g^{-1} after 7000 cycles at 5 A g^{-1} (99% capacity retention rate). Moreover, it still maintained 154 mAh g^{-1} at a high current density of 15 A g^{-1}.

S doping is also of particular interest because S can reversibly react with sodium. Since S has a larger covalent radius, it can hold more Na^+ and promote the insertion/extraction process. Furthermore, N and S co-doping can synergistically promote the electrochemical performance of carbon-based materials [92, 101]. Bao et al. [102] synthesized flexible N- and S-doped CNFs (NSCNFs) using urea as the S source (Fig. 4b). The flexible NSCNF film exhibited excellent rate performance and long cycle life, and the capacity retention was 90.8% at 10 A g^{-1} after 6000 cycles. Sun et al. [103] introduced S atoms to N-doped carbons to obtain S-enriched N-doped hollow CNF films (NSCNF) through electrospinning combined with heat treatment. As a flexible binder-free anode, NSCNF delivered a reversible capacity of 336.2 mAh g^{-1} at 0.05 A g^{-1}, and even maintained a capacity of 187 mAh g^{-1} at 2 A g^{-1} over 2000 cycles. Density functional theory calculations showed that the prepared sample not only promotes the adsorption of Na^+, but also facilitates the transfer of electrons. This strategy has been proven to be a general process for designing flexible heteroatom-doped carbon film electrodes with good Na^+ storage performance.

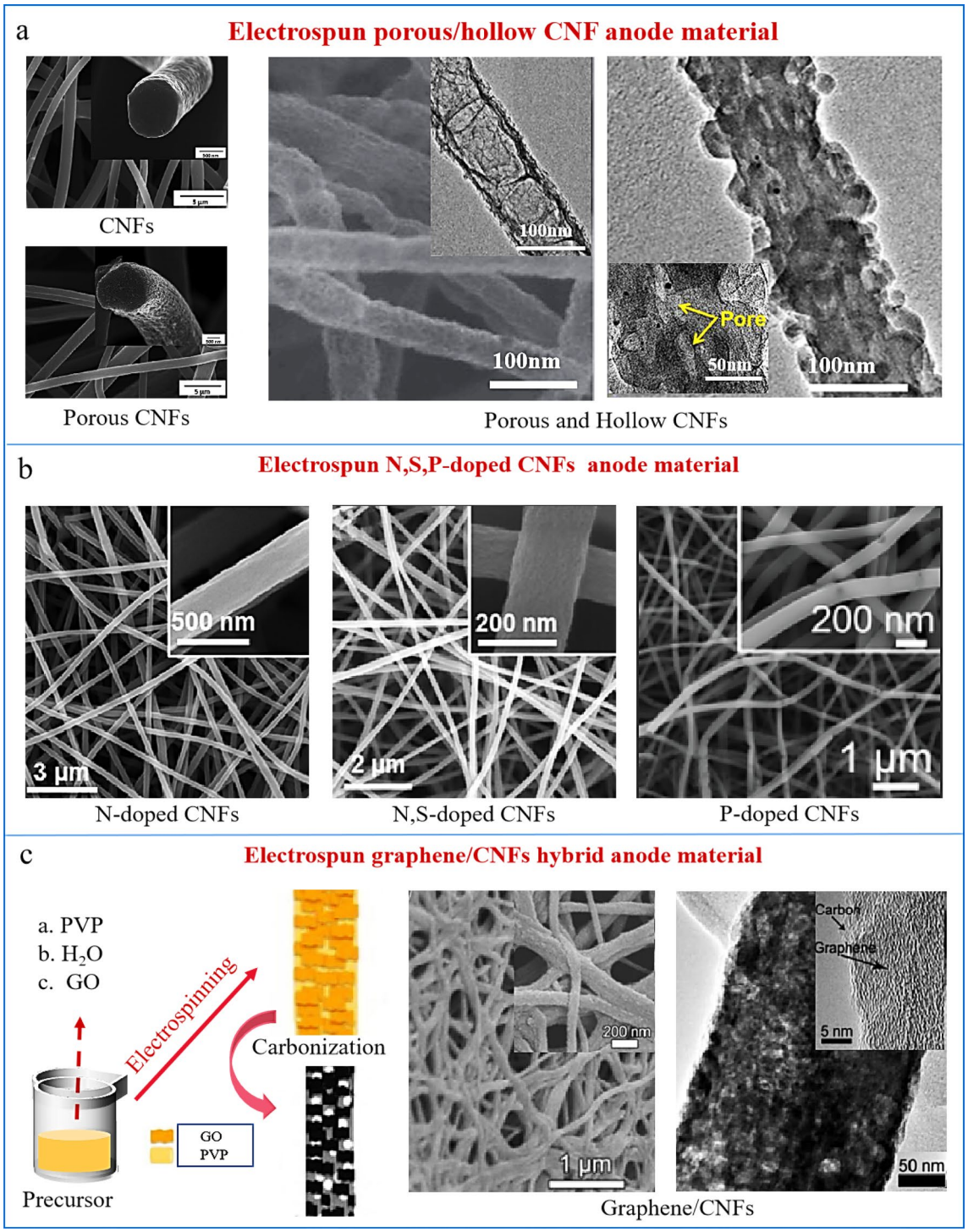

Fig. 4 Synthesis of electrospun carbonaceous anode material. **a** SEM images of CNFs and porous CNFs, porous and hollow CNFs. Reproduced with permission [86]. Copyright 2016, Elsevier. Reproduced with permission [47]. Copyright 2017, Elsevier. **b** SEM images of N-doped CNFs, N,S-doped CNFs, and P-doped CNFs. Reproduced with permission [102]. Copyright 2018, Elsevier. Reproduced with permission [106]. Copyright 2018, American Chemical Society. **c** Schematic illustration of the synthetic process and SEM and TEM images of graphene/CNFs. Reproduced with permission [24]. Copyright 2017, Royal Society of Chemistry

Besides S and N doping, considerable attention has also been paid to phosphorus (P) doping because of the P–C bond formed and large interlayer spacing, which can also yield more Na^+ adsorption/desorption in carbonaceous electrodes [104]. Li et al. [105] synthesized phosphorus-functionalized hard carbon (PHC) with a "honeycomb" structure by electrospinning. It was found that the prepared PHC showed a high capacity of 393.4 mAh g^{-1} after 100 cycles at 20 mA g^{-1} with a capacity retention rate as high as 98.2%. Wu et al. used H_3PO_4 as the phosphorus precursor to synthesize P-doped microporous electrospun CNFs [106]. The prepared P-doped CNFs showed a high reversible capacity of 288 mAh g^{-1}, which was higher than that of CNFs (239 mAh g^{-1}).

Hybrid Carbon 2D nanostructured graphene has large specific surface area, good flexibility, high chemical stability, and excellent electronic conductivity, and consequently, has received considerable attention for energy conversion and storage applications. Integrating CNF and graphene to form a hybrid is an effective way to further enhance the performance of CNFs. Liu, Fan and Jiao [24] dispersed monolayer (bilayer) graphene into porous CNFs by electro-spinning (Fig. 4c) to form a free-standing flexible anode, which showed a high reversible capacity of 432.3 mAh g^{-1} at 100 mA g^{-1}, an excellent rate capability of 261.1 mAh g^{-1} even at 10 A g^{-1} and an ultra-long cycle life with 91% capacity retention after 1000 cycles. The exceptional performance was attributed to the synergy between the porous CNFs and the highly exfoliated graphene layers, which could provide a large number of active sites and open ion diffusion channels to ensure sufficient electrolyte penetration and transport of ions and electrons.

Carbon/Alloy Composite Anodes

Alloy materials such as Sn and Sb are considered promising anode candidates for SIBs due to their high theoretical specific capacities. However, volume changes during cycling are dramatic. Nanostructure engineering is beneficial to ion and electron transport. Furthermore, it can accommodate the volume change of active materials during cycling. Additionally, the introduction of carbon to alloys not only enhances the conductivity but serves as a buffer to alleviate the stress. Below we will discuss how alloy materials can be confined in the electrospun carbon substrate in order to obtain composite anodes for SIBs.

Alloy Nanoparticles in Solid CNFs 1D CNFs are a promising matrix because of their 1D nanostructure and high conductivity, which facilitate electron and ion transport and effectively accommodate the large volume change of the alloys during repeated cycling. Zhu et al. [107] used electrospinning technology to prepare Sb nanoparticles with a diameter of 30 nm uniformly encapsulated in 1D interconnected CNFs with a diameter of ~ 400 nm (Fig. 5a). The initial capacity of the prepared Sb/C electrode was 422 mAh g^{-1} and maintained 350 mAh g^{-1} after 300 cycles. Similarly, Wu et al. [108] synthesized Sb/C nanofibers by single-nozzle electrospinning and subsequent carbothermal reaction, where Sb nanoparticles were evenly distributed within the CNFs (Fig. 5a). The fabricated Sb/C electrode displayed a high reversible capacity of 631mAh g^{-1} at a rate of C/15 (1C = 600 mA g^{-1}), and the capacity retention rate was 90% after over 400 cycles at C/3. Bi has also been studied widely as the alloy anode for SIBs. Yin et al. [109] prepared a uniform structure of Bi/C nanofibers, which showed a capacity of 273.2 mAh g^{-1} after 500 cycles at 100 mA g^{-1}. Inspired by the spider web structure, Jin et al. [110] prepared a spider web-like Bi/C membrane by electrospinning. When used as anodes, the membrane showed a good rate performance and cycle stability with a high reversible capacity of 186 mAh g^{-1} at 50 mA g^{-1} after 100 cycles. Kim and Kim [111] combined two alloys of Sn and Sb into an electrospun carbon matrix to obtain the hybrid fibers (Fig. 5a). Owing to the synergistic effect of the nanostructure, the fabricated electrode delivered a capacity of 385 mAh g^{-1} at a current density of 50 mA g^{-1}. To further enhance the structural integrity and conductivity of the substrate, Jia et al. [112] used reduced graphene oxide (RGO)/CNF hybrid as the substrate to obtain the SnSb/RGO/CNF composite. The composite material displayed high electrical conductivity and buffered efficiently volume changes. As an anode, the material showed a high capacity of 490 mAh g^{-1}. Like RGO, metal doping is also an efficient way to improve the structural integrity and conductivity of the matrix. Kim and Kim [113] used double-nozzle electrospinning technology to introduce Cu into Sn/C to obtain the Cu/Sn/C composite fiber (Fig. 5a). After 200 cycles, the electrode still showed a high reversible capacity of 220 mAh g^{-1}. In addition, incorporating highly stable electrochemical materials, e.g., TiO_2, is also beneficial for structural stability. Mao et al. [114] integrated high-capacity Sn, highly electrochemical-stable TiO_2, and high-conductivity CNF to obtain the fiber-in-tube structure with Sn/CNF as the core and TiO_2 as the shell. The outer TiO_2 coating on the Sn/CNF served as a protective shell to suppress Sn volume changes. The CNF not only improved the conductivity but also prevent Sn pulverization. The prepared anode showed a capacity of 413 mAh g^{-1} after 400 cycles at 100 mA g^{-1} (Fig. 5a).

Alloy Nanoparticles in Porous CNFs Porous structure is of great significance in improving the cycle life of alloys because it can provide ample space to accommodate the large volume changes of alloys during cycling. Ji et al. [115] used electrospinning and subsequent heat treatment to pre-

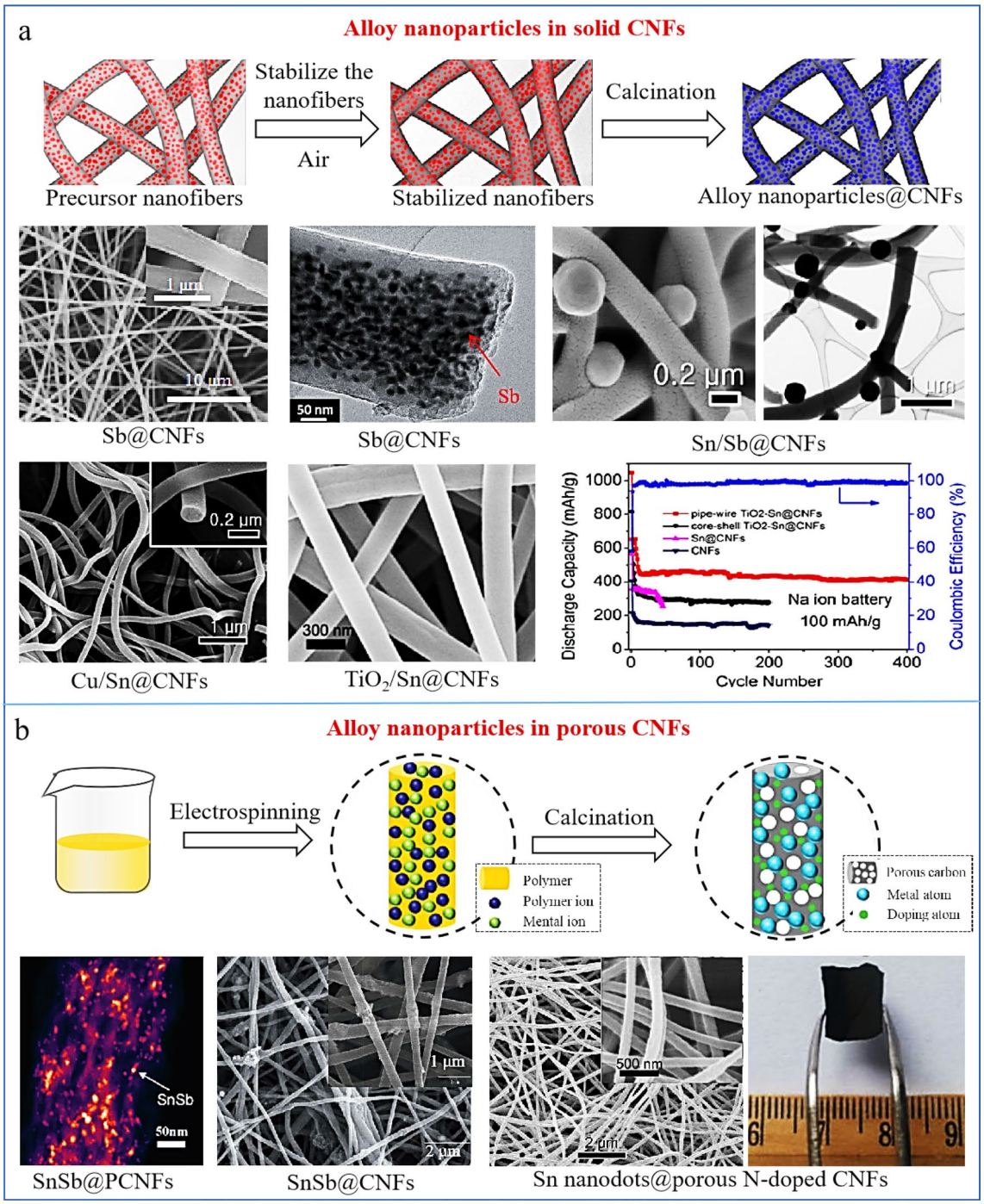

Fig. 5 Synthesis of electrospun alloy anode materials. **a** Preparation process of solid CNFs combined with alloy nanoparticles, SEM and TEM images of Sb/CNFs, Sn/Sb/CNFs, Cu/Sn/CNFs and TiO_2/Sn/CNFs, and cycle stability of CNFs with different alloy composite components. Reproduced with permission [107]. Copyright 2013, American Chemical Society. Reproduced with permission [107]. Copyright 2014, Royal Society of Chemistry. Reproduced with permission [108]. Copyright 2014, Elsevier. Reproduced with permission [111]. Copyright 2014, Wiley–VCH. Reproduced with permission [114]. Copyright 2017, American Chemical Society. **b** Two-step method combined electrospinning with calcination to synthesize porous CNFs combined with alloy nanoparticles, image illustration of SnSb/PCNFs, SnSb/CNFs and Sn nanodots/porous N-doped CNFs. Reproduced with permission [115]. Copyright 2014, Wiley–VCH. Reproduced with permission [116]. Copyright 2015, Royal Society of Chemistry. Reproduced with permission [117]. Copyright 2015, Wiley–VCH

pare porous CNFs to support tin antimonide nanoparticles (Fig. 5b), and the final electrode delivered a high reversible capacity of about 350 mAh g^{-1} with an excellent capacity retention rate of 99.4% after 200 cycles, and a high reversible capacity of 110 mAh g^{-1} at 10,000 mA g^{-1}. Chen et al. [116] processed a Sn–Sb alloy in porous CNFs by electrospinning and heat treatment (Fig. 5b). The porous structure of the composite material provided free space to alleviate the volume changes during sodium insertion and removal. The fabricated electrode gave a high capacity of 590 mAh g^{-1} at 50 mA g^{-1}; when the current density was increased to 1 A g^{-1}, it still showed a high capacity of 370 mAh g^{-1}. Heteroatom doping (such as N, S, B, and P) can adjust the conductivity of carbon materials and improve their electrochemical performance. Therefore, heteroatom-doped 1D nanocarbon as alloy substrate has triggered extensive research interest. Liu et al. [117] used electrospinning to evenly embed ultra-small tin nano-dots (1–2 nm) in porous N-doped CNFs (Fig. 5b). The size and content of the Sn particles could be adjusted by controlling the carbonization temperature and time. The obtained binder-free electrode yielded a capacity of 633 mAh g^{-1} at a current density of 200 mA g^{-1}. Even at a high rate of 2000 mA g^{-1}, a capacity of 483 mAh g^{-1} can be maintained after 1300 cycles.

Carbon/Metal Oxide Composite Anodes

Metal oxides are also promising anodes for SIBs because of their high theoretical capacities and natural abundance. However, metal oxides undergo severe volume changes during cycling. Such a large volume change leads to serious pulverization of active materials and reduces the electrical contact between the current collector and active materials, resulting in rapid capacity loss. Additionally, metal oxides show low conductivity, which limits their rate performance. Carbon has been proved as an excellent skeleton for metal oxides. It cannot only enhance the electrode conductivity but serve as a buffer to alleviate the strain produced during the charging and discharging processes. The typical fabrication process of electrospun carbon/metal oxide composites is illustrated in Fig. 6a.

Metal Oxide Nanoparticles in CNFs Xu et al. [118] synthesized amorphous FeO_x particles embedded in CNF films with a reversible capacity of 277 mAh g^{-1} (Fig. 6b). To

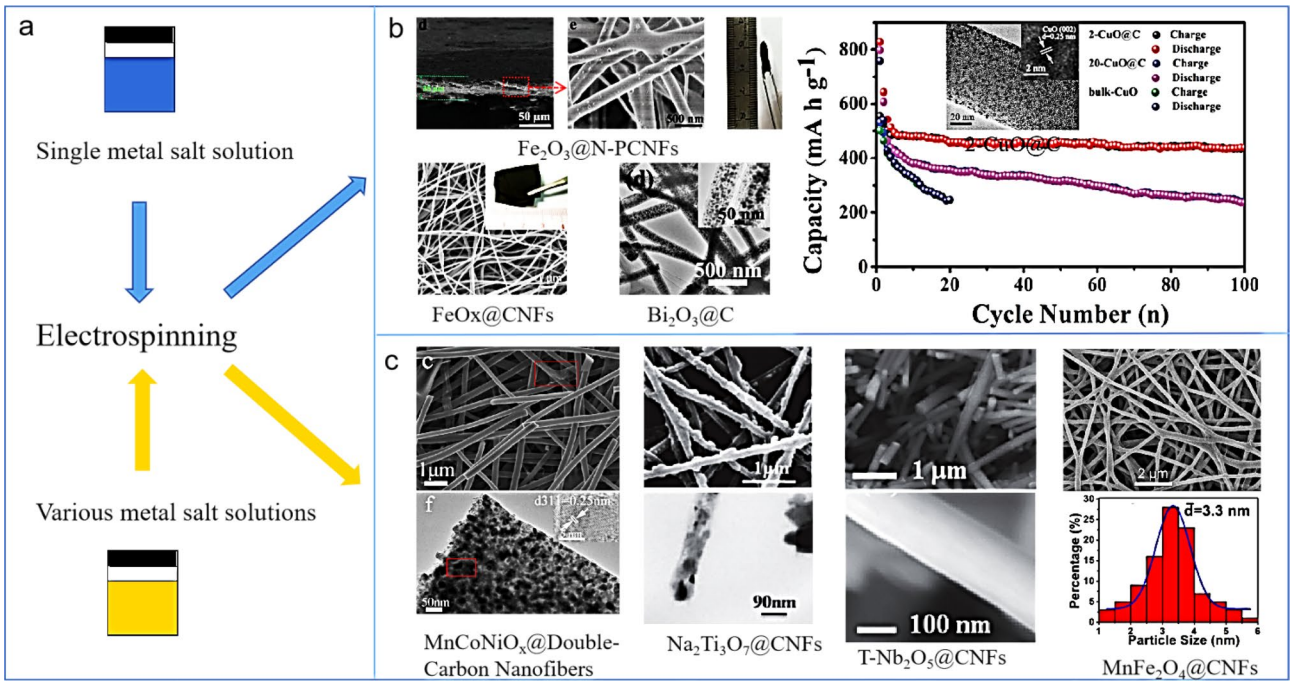

Fig. 6 Synthesis of electrospun metal oxide nanoparticles anode materials. **a** Fabrication of two types of metal oxide composite CNFs. **b** Image illustrations of Fe_2O_3@N-PCNFs, FeO_x@CNFs, Bi_2O_3@C, 2-CuO@C, and cycle stability of different CuO/C ratios. Reproduced with permission [119]. Copyright 2017, Wiley–VCH. Reproduced with permission [118]. Copyright 2017, Elsevier. Reproduced with permission [120]. Copyright 2017, Royal Society of Chemistry. Reproduced with permission [124]. Copyright 2016, Wiley–VCH. **c** Image illustrations of $MnCoNiO_x$@double-carbon nanofibers, $Na_2Ti_3O_7$@CNFs, T-Nb_2O_5@CNFs and $MnFe_2O_4$@CNFs; and $MnFe_2O_4$ particle size distribution diagram. Reproduced with permission [121]. Copyright 2016, American Chemical Society. Reproduced with permission [122]. Copyright 2017, Wiley–VCH. Reproduced with permission [123]. Copyright 2017, Wiley–VCH. Reproduced with permission [99]. Copyright 2016, American Chemical Society

pursue excellent rate capability and cycling stability, Xia et al. [119] synthesized a 3D composite material composed of Fe_2O_3 nanoparticles embedded in N-doped porous CNFs (Fe_2O_3/N-PCNFs) for use as flexible electrodes (Fig. 6b). This unique structure not only provided enough voids to accommodate the volume expansion of Fe_2O_3 nanoparticles but also offered a successive conducting framework for electron transport and accessible channels for rapid diffusion and transport of Na^+. Hence, the material delivered a steady discharge capacity of 806 mAh g^{-1} at 200 mA g^{-1} after 100 cycles. Importantly, a stable capacity of 396 mAh g^{-1} could be reached at a high current density of 2000 mA g^{-1} after 1500 cycles. Bismuth oxide (Bi_2O_3) is also an excellent anode due to its stable chemical properties, a high theoretical capacity of 669.8 mAh g^{-1}, and environmental friendliness. Yin et al. [120] embedded Bi_2O_3 nanoparticles in CNFs to prepare a flexible film (Fig. 6b). The electrode showed a special rate capability of 230 mAh g^{-1} at 3200 mA g^{-1} and a high reversible capacity of 430 mAh g^{-1} after 200 cycles at 100 mA g^{-1}.

Besides the mono-metal oxides, multi-metal oxides nanoparticles are also regarded as a good anode for SIBs (Fig. 6a). Wu et al. [121] successfully synthesized $MnCoNiO_x$ nanocrystals (< 30 nm) in CNFs (MCNO@CNF) as shown in Fig. 6c. The prepared MCNO@CNF composite displayed a particularly high specific capacity of 230 mAh g^{-1} at 0.1 A g^{-1} after 500 cycles, and a specific capacity of 107 mAh g^{-1} at 1 A g^{-1} after 6500 cycles. Their excellent electrochemical performance was mainly attributed to the small MCNO nanoparticles, shortening the Na^+ diffusion distance, while the 3D fibrous framework significantly enhanced the electronic transport and effectively limited collapse caused by the volume fluctuation of the MCNO nanoparticles during the charge and discharge process. Zou, Fan and Li [122] used PVP additive to control the diameter of the composite fiber and fabricated $Na_2Ti_3O_7$/C nano-fibers with fiber diameter ~ 140 nm and $Na_2Ti_3O_7$ particle size ~ 40 nm (Fig. 6c), delivering the high capacities of 195 and 101 mAh g^{-1} at 0.1 C and 4 C (1C = 178 mA g^{-1}), respectively. Recently, Yang et al. [123] reported a new type of T-Nb_2O_5/CNFs composite material with ultra-small T-Nb_2O_5 nanoparticles (about 6–8 nm) encapsulated in CNFs through electrospinning and pyrolysis treatment (Fig. 6c). Due to the engineering of the micro-nano structure and the ideal pseudo-sensitization behavior of T-Nb_2O_5, T-Nb_2O_5/CNFs achieved a high capacity of 150 mAh g^{-1} at 1 A g^{-1} after 5000 cycles.

To resolve the severe volume changes of metal oxides during cycling, another method is to further decrease the size of metal oxides (< 5 nm), like nanodots in CNFs, which can enhance the performance of anode materials. Wang et al. [124] reported the preparation of CuO quantum dots (≈ 2 nm) uniformly distributed in solid CNFs (2-CuO@C) as a freestanding anode for SIBs, which delivered a high reversible capacity of 528 mAh g^{-1} at 100 mA g^{-1} and long cycling stability of 401 mAh g^{-1} at 500 mA g^{-1} after 500 cycles (Fig. 6b). The high electrochemical performance was mainly attributed to the ultra-small quantum dots, which effectively shortened the ionic diffusion paths and prompted the conversion reaction. Also, Liu, Wang and Fan [125] prepared ultra-small Fe_2O_3 nanodots (~ 3.4 nm) packaged in porous N-doped CNFs (Fe_2O_3@PNCNF) by electrospinning. The prepared electrode exhibited a reversible capacity of 345 mAh g^{-1} with a capacity retention of 98.3% after 1000 cycles. Liu et al. [99] reported the preparation of $MnFe_2O_4$ nanodots (~ 3.3 nm) in porous N-doped CNFs (MFO@PNCNF), as displayed in Fig. 6c. When used as the anodes, MFO@PNCNF displayed an excellent electrochemical performance in terms of high rate performance (391 mAh g^{-1} at 2000 mA g^{-1}) and long cycle life (90% capacity retention after 4200 cycles). Furthermore, the full cell composed of MFO@PNCNF anode and $Na_3V_2(PO_4)_2F_3$/C cathode showed a high energy density of 77.8 Wh kg^{-1}.

Carbon/Metal Sulfide Composite Anodes

Metal sulfides based on conversion reaction mechanisms with high theoretical capacity have attracted great attention for SIBs. For example, carbon-coated Sb_2S_3 nanorods provided new clues for the development of high-performance anodes for SIBs [126]. Hayashi et al. [127] synthesized a sodium-ion sulfide conductor $Na_{2.88}Sb_{0.88}W_{0.12}S_4$, in which Sb in Na_3SbS_4 was partially replaced by W, hence introducing sodium vacancies and the cubic phase transition. As a result, $Na_{2.88}Sb_{0.88}W_{0.12}S_4$ had the highest room temperature conductivity of 32 mS cm^{-1}. However, metals sulfides suffer from sluggish Na^+ diffusion kinetics, low electrical conductivity, and severe volume variation during cycling resulting in inferior rate and cycle performance. Their hybrids with carbon represent a common approach to enhance the reaction kinetics and electrochemical performance.

Metal Sulfide in CNFs Molybdenum disulfide (MoS_2) is a layered transition metal disulfide in which a hexagonal molybdenum layer is sandwiched between two sulfur layers [128–131]. Because of its obvious redox variability and structural characteristic, it is a good host for Na^+. However, the MoS_2 electrode suffers from rapid capacity attenuation and low rate performance due to the conversion reaction mechanisms and low electronic conductivity. Introduction of carbon into MoS_2 has been proven an effective strategy to address these issues (Fig. 7a) [132]. A typical example was reported by Zhu et al. who embedded a single-layer MoS_2 nano-plate (0.4 nm in thickness and 4 nm in length) in CNFs through electrospinning (Fig. 7a) [133]. The unique structure enabled the fast reaction of high-activity MoS_2 with

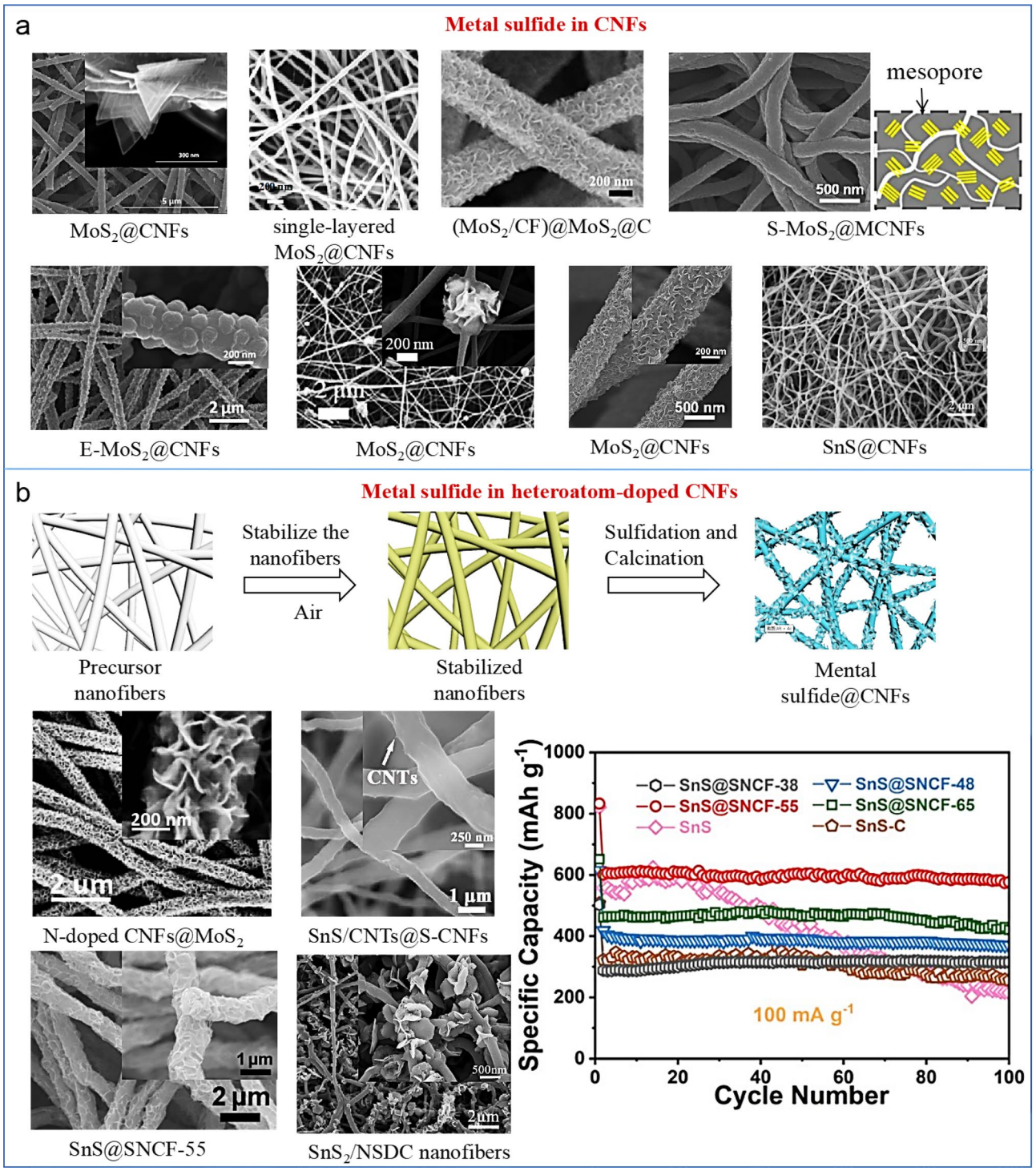

Fig. 7 Synthesis of electrospun metal sulfide anode materials. Image illustrations of MoS_2@CNFs, single-layered MoS_2@CNFs, (MoS_2/CF)@MoS_2@C, S-MoS_2@MCNFs, E-MoS_2@CNFs, MoS_2@CNFs, MoS_2@CNFs, and SnS@CNFs. Reproduced with permission [132]. Copyright 2016, Elsevier. Reproduced with permission [133]. Copyright 2014, Wiley–VCH. Reproduced with permission [134]. Copyright 2018, Elsevier. Reproduced with permission [135]. Copyright 2016, American Chemical Society. Reproduced with permission [136]. Copyright 2017, Elsevier. Reproduced with permission [137]. Copyright 2019, American Chemical Society. Reproduced with permission [138]. Copyright 2018, American Chemical Society. Reproduced with permission [139]. Copyright 2019, Elsevier. **b** Preparation process of heteroatom-doped CNFs combined with alloy nanoparticles, SEM image of N-doped CNFs@MoS_2, SnS/CNTs@S-CNFs, SnS@SNCF-55, SnS_2/NSDC nanofibers, and cycle stability of different SnS/C ratio. Reproduced with permission [145]. Copyright 2019, Elsevier. Reproduced with permission [141]. Copyright 2018, Elsevier. Reproduced with permission [143]. Copyright 2018, Elsevier. Reproduced with permission [144]. Copyright 2019, Elsevier

Na^+, which effectively alleviates the structural instability and poor reversibility. The obtained electrode showed a specific capacity of 854 mAh g^{-1} at a current density of 0.1 A g^{-1}, and a capacity of 253 mAh g^{-1} can be maintained even at 10 A g^{-1} after 100 cycles. Cui et al. [134] synthesized MoS_2@C hybrids through combined electrospinning, hydrothermal and annealing (Fig. 7a). Considering the high MoS_2 content (75.3 wt%), the electrode provided a large initial capacity of 773.5 mAh g^{-1} at 100 mA g^{-1}. After 1000 cycles, it maintained a high reversible capacity of 332.6 mA g^{-1} at 1 A g^{-1}. Jung et al. [135] synthesized several layers of MoS_2 nano-plates embedded in mesoporous CNFs (MoS_2@MCNFs) (Fig. 7a). The prepared MoS_2@MCNFs had a relatively large interlayer spacing and a shortened lateral distance, yielding long cycle life and excellent rate performance. Zhao et al. [136] prepared novel MoS_2 nano-particles with swelling and ultra-wide interlayer spacing on CNFs (Fig. 7a). The layer spacing was almost twice that of original MoS_2 which increased the ion diffusion pathways. Therefore, the prepared MoS_2/CNF delivered a capacity of 104 mAh g^{-1} at 20 A g^{-1}. Recently, Ni et al. [137] developed an in-situ electrospinning method to prepare MoS_2-based flexible electrodes (Fig. 7a) which had higher electronic conductivity and ion diffusion coefficient than those of pure MoS_2. It exhibited a significantly high specific capacity of 596 mAh g^{-1} at 50 mA g^{-1}, and the capacity retention rate was 89% at 1 A g^{-1} after 1100 cycles. Additionally, Li et al. [138] directly prepared 3D flexible interconnection MoS_2 with extended interlayer spacing epitaxial on electrospun CNF (MoS_2@CNF) (Fig. 7a). The C–O–Mo bond promoted the charge transfer. Consequently, the flexible MoS_2@CNFs electrode exhibited a significant specific capacity (528 mAh g^{-1} at 100 mA g^{-1}), excellent rate performance (412 mAh g^{-1} at 1 A g^{-1}), and long life (over 600 cycles at 1 A g^{-1}). These processes can also be used to integrate other metal sulfides and carbon. Hence, Xia et al. [139] proposed a free-standing SnS/carbon composite nanofiber membrane with a reversible capacity of 481 mAh g^{-1} at 50 mA g^{-1} (Fig. 7a). In addition, Chen et al. [140] also synthesized exfoliated MoS_2@C nanosheets as an anode for SIBs, which showed a high capacity of 641 mAh g^{-1} at 50 mA g^{-1} and still maintained a capacity of 214 mAh g^{-1} at 1000 mA g^{-1} after 400 cycles.

Metal Sulfide in Heteroatom-Doped CNFs Heteroatom doping increases the actives sites and the electronic/ionic conductivity of the carbon substrate. A typical example was made by Liang et al. [141] who introduced N-doped CNF as a substrate for MoS_2. More interestingly, they also introduced S vacancies into the N-doped CNF@MoS_2 nanosheet array (Fig. 7b), and the discharge capacity was 495 mAh g^{-1} at 100 mA g^{-1}. Theoretical calculations showed that S vacancies acted as new active centers to promote the adsorption of Na^+ and the conductivity, which was in good agreement with the experimental results. In addition to MoS_2, SnS also has a layered structure similar to graphene, and the atomic layers are held together by van der Waals force, which makes Na^+ easily to intercalate and delaminate [142]. To overcome problems such as volume change, low conductivity, and slow alkalization kinetics, the S-doped CNFs and CNTs were used as the substrate to form SnS/CNT@S-CNFs (Fig. 7b) [143]. Due to the flexible structure and enhanced conductivity, the prepared electrode provided a reversible capacity of 296.6 mAh g^{-1} at 0.8 A g^{-1} after 600 cycles. Furthermore, an excellent rate capability of 252.4 mAh g^{-1} was achieved at 3.2 A g^{-1}. Recently, Wang et al. [144] embedded SnS nanoparticles in (S, N) co-doped mesoporous CNFs (SnS@SNCF). Due to the synergistic effect of co-doping, the composite material exhibited a high specific capacity of 630 mAh g^{-1} at 0.1A g^{-1}, and there was almost no capacitance attenuation after 50 cycles. When the current density was increased to 1.6 A g^{-1}, a capacity of 400 mAh g^{-1} was maintained (Fig. 7b). Additionally, Xia et al. [145] not only embedded SnS_2 nanoparticles inside (N, S) co-doped CNFs (SnS_2/NSCNF) (Fig. 7b), but also grew some SnS_2 nano-sheets on the NSCNF to fabricate hierarchical core–shell structure. Owing to the unique structure, SnS_2/NSCNF exhibited excellent performance with a capacity of 380.1 mAh g^{-1} after 200 cycles at 500 mA g^{-1}.

Carbon/Vanadium-Based Composite Anodes

Vanadium and vanadium-based materials, as transition metal elements in different valence states (V^{2+}, V^{3+}, V^{4+}, and V^{5+}), are used in electrochemical energy storage due to their inherent simple synthesis process, low-cost, and large theoretical capacity [146]. Luo et al. [147] prepared Fe_2VO_4 hierarchical porous microparticles as anodes for SIBs, which delivered a high capacity of 229 mAh g^{-1} after 1000 cycles at 1 A g^{-1}. Recently, a new type of $VSe_{1.5}$/CNF composite material was processed by combining electrospinning and selenization. When used as an anode material for SIBs, $VSe_{1.5}$/CNF composite exhibited a high reversible capacity of 668 mAh g^{-1} after 50 cycles; and even after 6000 ultra-long cycles at 2 A g^{-1}, it exhibited an excellent capacity of 265 mAh g^{-1} (Fig. 8a, b) [148]. Xu et al. [149] initially designed and prepared a vanadium nitride/carbon fiber (VN/CNF) composite material using a simple electro-spinning method followed by an ammoniation process (Fig. 8b). The full battery assembled by VN/CNF composite anode and NVP cathode showed an ideal capacity of 257 mAh g^{-1} after 50 cycles under 500 mA g^{-1}.

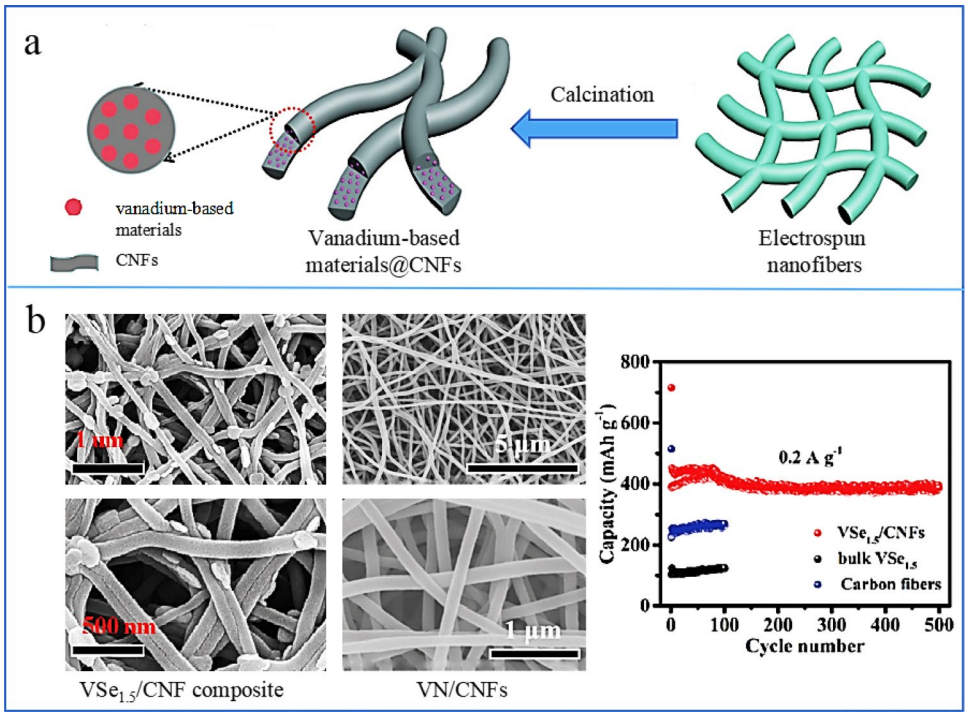

Fig. 8 Synthesis of electrospun vanadium-based anode material. **a** Preparation of CNFs combined with vanadium-based materials. **b** SEM images of $VSe_{1.5}$/CNF and VN/CNFs. Comparison of cycle stability between carbon fibers, bulk $VSe_{1.5,}$ and $VSe_{1.5}$/CNFs. Reproduced with permission [148]. Copyright 2019, Royal Society of Chemistry. Reproduced with permission [149]. Copyright 2020, Royal Society of Chemistry

Summary and Outlook

In this review, we have systematically examined the rational design and synthesis of 1D carbon-based nano-materials with various architectures and compositions by the electrospinning strategy. The synthetic process for these 1D nanomaterials can be well controlled by altering the electrospinning parameters and post-treatment. 1D electro-spun materials are one of the promising materials as cathodes and anodes for SIBs because 1D nanostructures provide adequate contact between electrode and electrolyte to boost the transport of ions and inhibit structural failure during iterative cycling, thus enhancing the cyclic stability and rate capability. Specifically, the electrospun carbon matrix not only increases the electrical conductivity of the entire electrode, but also serves as the buffer to alleviate the large strain of the active materials. Moreover, introduction of porous and hollow structures into electrospun nanomaterials can accommodate effectively the volume changes of the active materials, enabling enhanced structural stability. In addition, appropriate heteroatom doping of the carbon matrix also improves the electrical conductivity. This review aims to highlight the significant roles of electrospinning engineering to optimize the electrodes for high-performance SIBs.

Although the development of electrospun carbon-based electrodes has achieved substantial progress, there are still many challenges that need to be addressed. First, the initial coulombic efficiency (ICE) of the electrospun carbon-based electrodes for SIBs is usually low due to the formation of the solid electrolyte interphase (SEI) film and some side reactions between the electrolyte and electrode, stemming from the porous structure and high specific surface areas. The inferior ICE consumes large amounts of Na^+ from the cathode, leading to a waste of expensive cathodes in commercial applications. Thus, it is essential to prevent direct contact between electrode and electrolyte. Coating a passivated layer on the active materials is a promising method to address this issue. Second, mass production is an important indicator for practical applications. Despite electrospun electrodes with good Na^+ storage capacity have been reported, it is still a great challenge to strengthen electrode materials by the common electrospinning setup. The key to realizing mass production is to adopt multi-jets. Thus, it is of utmost importance to modify the nozzle. Multi-nozzle electrospinning, bubble electrospinning and needleless electrospinning can be used to generate nanofibers on a large and efficient scale. Third, the microstructure of the electrospun carbon-based materials (pore size, heteroatom doping, etc.) plays a vital role in determining the final electrochemical performance of SIBs. The pore size should be tailored to allow convenient access of Na^+. The heteroatom doping usually induces abundant defects and these defects need to be precisely tuned by optimizing the synthetic process.

References

1. Chen Y, Liu C, Sun X, Ye H, Cheung C, Zhou L. Recycled diesel carbon nanoparticles for nanostructured battery anodes. *J Power Sources*. **2015**;*275*:26.

2. Yabuuchi N, Kubota K, Dahbi M, Komaba S. Research development on sodium-ion batteries. *Chem Rev*. **2014**;*114*:11636.
3. Jamesh M-I. Recent advances on flexible electrodes for Na-ion batteries and Li–S batteries. *J Energy Chem*. **2019**;*32*:15.
4. Xu ZL, Park J, Yoon G, Kim H, Kang K. Graphitic carbon materials for advanced sodium-ion batteries. *Small Methods*. **2018**;*3*:1800227.
5. Kim S-W, Seo D-H, Ma X, Ceder G, Kang K. Electrode materials for rechargeable sodium-ion batteries: potential alternatives to current lithium-ion batteries. *Adv Energy Mater*. **2012**;*2*:710.
6. Kim H, Kim H, Ding Z, Lee MH, Lim K, Yoon G, Kang K. Recent progress in electrode materials for sodium-ion batteries. *Adv Energy Mater*. **2016**;*6*:1600943.
7. Komaba S, Takei C, Nakayama T, Ogata A, Yabuuchi N. Electrochemical intercalation activity of layered $NaCrO_2$ vs. $LiCrO_2$. *Electrochem Commun*. **2010**;*12*:355.
8. Wei Q, Xiong F, Tan S, Huang L, Lan EH, Dunn B, Mai L. Porous one-dimensional nanomaterials: design, fabrication and applications in electrochemical energy storage. *Adv Mater*. **2017**;*29*:1602300.
9. Zhang Q, Uchaker E, Candelaria SL, Cao G. Nanomaterials for energy conversion and storage. *Chem Soc Rev*. **2013**;*42*:3127.
10. Jin T, Han Q, Wang Y, Jiao L. 1D Nanomaterials: design, synthesis, and applications in sodium-ion batteries. *Small*. **2018**;*14*:1703086.
11. Subramanian V, Zhu H, Wei B. High rate reversibility anode materials of lithium batteries from vapor-grown carbon nanofibers. *J Phys Chem B*. **2006**;*110*:7178.
12. Cavaliere S, Subianto S, Savych I, Jones DJ, Rozière J. Electrospinning: designed architectures for energy conversion and storage devices. *Energy Environ Sci*. **2011**;*4*:4761.
13. Xue J, Xie J, Liu W, Xia Y. Electrospun nanofibers: new concepts, materials, and applications. *Acc Chem Res*. **1976**;*2017*:50.
14. Wang Z, Li X, Chen Y, Pei K, Mai Y-W, Zhang S, Li J. Creep-enabled 3D solid-state lithium-metal battery. *Chemistry*. **2020**;*6*:2878.
15. Li X, Chen W, Qian Q, Huang H, Chen Y, Wang Z, Chen Q, Yang J, Li J, Mai YW. Electrospinning-based strategies for battery materials. *Adv Energy Mater*. **2020**;*11*:2000845.
16. Zhao J, Hu Z, Chen S, Zhang W, Liu X. Electrospinning synthesis of amorphous $NiMoO_4$/graphene dendritic nanofibers as excellent anodes for sodium ion batteries. *Nanotechnology*. **2020**;*31*:505401.
17. Zhao W, Ma X, Gao L, Li Y, Wang G, Sun Q. Engineering carbon-nanochain concatenated hollow Sn_4P_3 nanospheres architectures as ultrastable and high-rate anode materials for sodium ion batteries. *Carbon*. **2020**;*167*:736.
18. Zhao W, Ma X, Li Y, Wang G, Long X. Achieving ultrastable cyclability and pseudocapacitive sodium storage in SnSe quantum-dots sheathed in nitrogen doped carbon nanofibers. *Appl Surf Sci*. **2020**;*504*:144455.
19. Lu Z, Zhai Y, Wang N, Zhang Y, Xue P, Guo M, Tang B, Huang D, Wang W, Bai Z, Dou S. FeS_2 nanoparticles embedded in N/S co-doped porous carbon fibers as anode for sodium-ion batteries. *Chem Eng J*. **2020**;*380*:122455.
20. Zhang W, Yue Z, Wang Q, Zeng X, Fu C, Li Q, Li X, Fang L, Li L. Carbon-encapsulated CoS_2 nanoparticles anchored on N-doped carbon nanofibers derived from ZIF-8/ZIF-67 as anode for sodium-ion batteries. *Chem Eng J*. **2020**;*380*:122548.
21. Luo L, Song J, Song L, Zhang H, Bi Y, Liu L, Yin L, Wang F, Wang G. Flexible conductive anodes based on 3D hierarchical Sn/NS-CNFs@rGO network for sodium-ion batteries. *Nano-Micro Lett*. **2019**;*11*:63.
22. Jeong SY, Ghosh S, Kim J-K, Kang D-W, Jeong SM, Kang YC, Cho JS. Multi-channel-contained few-layered $MoSe_2$ nanosheet/N-doped carbon hybrid nanofibers prepared using diethylenetriamine as anodes for high-performance sodium-ion batteries. *J Ind Eng Chem*. **2019**;*75*:100.
23. Ma X, Chen L, Ren X, Hou G, Chen L, Zhang L, Liu B, Ai Q, Zhang L, Si P, Lou J, Feng J, Ci L. High-performance red phosphorus/carbon nanofibers/graphene free-standing paper anode for sodium ion batteries. *J Mater Chem A*. **2018**;*6*:1574.
24. Liu Y, Fan L-Z, Jiao L. Graphene highly scattered in porous carbon nanofibers: a binder-free and high-performance anode for sodium-ion batteries. *J Mater Chem A*. **2017**;*5*:1698.
25. Chen W, Zhang L, Liu C, Feng X, Zhang J, Guan L, Mi L, Cui S. Electrospun flexible cellulose acetate-based separators for sodium-ion batteries with ultralong cycle stability and excellent wettability: the role of interface chemical groups. *ACS Appl Mater Interfaces*. **2018**;*10*:23883.
26. Ray SS, Chen S-S, Li C-W, Nguyen NC, Nguyen HT. A comprehensive review: electrospinning technique for fabrication and surface modification of membranes for water treatment application. *RSC Adv*. **2016**;*6*:85495.
27. Sill TJ, von Recum HA. Electrospinning: applications in drug delivery and tissue engineering. *Biomaterials*. **1989**;*2008*:29.
28. Wang Y, Liu Y, Liu Y, Shen Q, Chen C, Qiu F, Li P, Jiao L, Qu X. Recent advances in electrospun electrode materials for sodium-ion batteries. *J Energy Chem*. **2021**;*54*:225.
29. Yarin AL, Koombhongse S, Reneker DH. Taylor cone and jetting from liquid droplets in electrospinning of nanofibers. *J Appl Phys*. **2001**;*90*:4836.
30. Lu Z, Sui F, Miao Y-E, Liu G, Li C, Dong W, Cui J, Liu T, Wu J, Yang C. Polyimide separators for rechargeable batteries. *J Energy Chem*. **2021**;*58*:170.
31. Xu M, Wang M, Xu H, Xue H, Pang H. Electrospun-technology-derived high-performance electrochemical energy storage devices. *Chem Asian J*. **2016**;*11*:2967.
32. Ekabutr P, Klinkajon W, Sangsanoh P, Chailapakul O, Niamlang P, Khampieng T, Supaphol P. Electrospinning: a carbonized gold/graphene/PAN nanofiber for high performance biosensing. *Anal Methods*. **2018**;*10*:874.
33. Sun B, Duan B, Yuan X. Preparation of core/shell PVP/PLA ultrafine fibers by coaxial electrospinning. *J Appl Polym Sci*. **2006**;*102*:39.
34. Bhardwaj N, Kundu SC. Electrospinning: a fascinating fiber fabrication technique. *Biotechnol Adv*. **2010**;*28*:325.
35. Islam MS, Ang BC, Andriyana A, Afifi AM. A review on fabrication of nanofibers via electrospinning and their applications. *SN Appl Sci*. **2019**;*1*:1248.
36. Li X, Chen W, Qian Q, Huang H, Chen Y, Wang Z, Chen Q, Yang J, Li J, Mai YW. Electrospinning-based strategies for battery materials. *Adv Energy Mater*. **2021**;*11*:2000845.
37. Zhang M, Huang X, Xin H, Li D, Zhao Y, Shi L, Lin Y, Yu J, Yu Z, Zhu C, Xu J. Coaxial electrospinning synthesis hollow Mo_2C@C core-shell nanofibers for high-performance and long-term lithium-ion batteries. *Appl Surf Sci*. **2019**;*473*:352.
38. Xue J, Wu T, Dai Y, Xia Y. Electrospinning and electrospun nanofibers: methods, materials, and applications. *Chem Rev*. **2019**;*119*:5298.
39. Liu C, Shi G, Wang G, Mishra P, Jia S, Jiang X, Zhang P, Dong Y, Wang Z. Preparation and electrochemical studies of electrospun phosphorus doped porous carbon nanofibers. *R Soc Chem Adv*. **2019**;*9*:6898.
40. Wu J, Qin X, Miao C, He Y-B, Liang G, Zhou D, Liu M, Han C, Li B, Kang F. A honeycomb-cobweb inspired hierarchical core–shell structure design for electrospun silicon/carbon fibers as lithium-ion battery anodes. *Carbon*. **2016**;*98*:582.
41. Chen Z, Yang T, Shi H, Wang T, Zhang M, Cao G. Single nozzle electrospinning synthesized MoO_2@C core shell nanofibers with

high capacity and long-term stability for lithium-ion storage. *Adv Mater Interfaces*. **2017**;*4*:1600816.
42. Shan C, Feng X, Yang J, Yang X, Guan H-Y, Argueta M, Wu X-L, Liu D-S, Austin DJ, Nie P, Yue Y. Hierarchical porous carbon pellicles: electrospinning synthesis and applications as anodes for sodium-ion batteries with an outstanding performance. *Carbon*. **2020**;*157*:308.
43. Li W, Zeng L, Yang Z, Gu L, Wang J, Liu X, Cheng J, Yu Y. Free-standing and binder-free sodium-ion electrodes with ultralong cycle life and high rate performance based on porous carbon nanofibers. *Nanoscale*. **2014**;*6*:693.
44. Chen Y, Dong J, Qiu L, Li X, Li Q, Wang H, Liang S, Yao H, Huang H, Gao H, Kim J-K, Ding F, Zhou L. A catalytic etching-wetting-dewetting mechanism in the formation of hollow graphitic carbon fiber. *Chemistry*. **2017**;*2*:299.
45. Chen Y, Li X, Park K, Zhou L, Huang H, Mai YW, Goodenough JB. Hollow nanotubes of N-doped carbon on CoS. *Angew Chem Int Ed Engl*. **2016**;*55*:15831.
46. Chen YM, Yu L, Lou XW. Hierarchical tubular structures composed of Co_3O_4 hollow nanoparticles and carbon nanotubes for lithium storage. *Angew Chem Int Ed Engl*. **2016**;*55*:5990.
47. Chen Y, Li X, Park K, Lu W, Wang C, Xue W, Yang F, Zhou J, Suo L, Lin T, Huang H, Li J, Goodenough JB. Nitrogen-doped carbon for sodium-ion battery anode by self-etching and graphitization of bimetallic MOF-based composite. *Chemistry*. **2017**;*3*:152.
48. Li X, Li K, Zhu S, Fan K, Lyu L, Yao H, Li Y, Hu J, Huang H, Mai YW, Goodenough JB. Fiber-in-tube design of Co_9S_8-Carbon/Co_9S_8: enabling efficient sodium storage. *Angew Chem Int Ed Engl*. **2019**;*58*:6239.
49. Ma M, Yao Y, Wu Y, Yu Y. Progress and prospects of transition metal sulfides for sodium storage. *Adv Fiber Mater*. **2020**;*2*:314.
50. Wang L, Yang G, Peng S, Wang J, Yan W, Ramakrishna S. One-dimensional nanomaterials toward electrochemical sodium-ion storage applications via electrospinning. *Energy Storage Mater*. **2020**;*25*:443.
51. Chen S, Wu C, Shen L, Zhu C, Huang Y, Xi K, Maier J, Yu Y. Challenges and perspectives for NASICON-type electrode materials for advanced sodium-ion batteries. *Adv Mater*. **2017**;*29*:1700431.
52. Xu Y, Wei Q, Xu C, Li Q, An Q, Zhang P, Sheng J, Zhou L, Mai L. Layer-by-layer $Na_3V_2(PO_4)_3$embedded in reduced graphene oxide as superior rate and ultralong-life sodium-ion battery cathode. *Adv Energy Mater*. **2016**;*6*:1600389.
53. Liu J, Tang K, Song K, van Aken PA, Yu Y, Maier J. Electrospun $Na_3V_2(PO_4)_3$/C nanofibers as stable cathode materials for sodium-ion batteries. *Nanoscale*. **2014**;*6*:5081.
54. Kajiyama S, Kikkawa J, Hoshino J, Okubo M, Hosono E. Assembly of $Na_3V_2(PO_4)_3$ nanoparticles confined in a one-dimensional carbon sheath for enhanced sodium-ion cathode properties. *Chemistry*. **2014**;*20*:12636.
55. Li H, Bai Y, Wu F, Ni Q, Wu C. $Na_3V_2(PO_4)_3$/C nanorods as advanced cathode material for sodium ion batteries. *Solid State Ionics*. **2015**;*278*:281.
56. Li H, Bai Y, Wu F, Li Y, Wu C. Budding willow branches shaped $Na_3V_2(PO_4)_3$/C nanofibers synthesized via an electrospinning technique and used as cathode material for sodium ion batteries. *J Power Sources*. 2015;273:784.
57. Yang L, Wang W, Hu M, Shao J, Lv R. Ultrahigh rate binder-free $Na_3V_2(PO_4)_3$/carbon cathode for sodium-ion battery. *J Energy Chem*. **2018**;*27*:1439.
58. Ni Q, Bai Y, Li Y, Ling L, Li L, Chen G, Wang Z, Ren H, Wu F, Wu C. 3D electronic channels wrapped large-sized $Na_3V_2(PO_4)_3$ as flexible electrode for sodium-ion batteries. *Small*. **2018**;*14*:1702864.
59. Li M, Liu L, Wang P, Li J, Leng Q, Cao G. Highly reversible sodium-ion storage in $NaTi_2(PO_4)_3$/C composite nanofibers. *Electrochim Acta*. **2017**;*252*:523.
60. Yu S, Wan Y, Shang C, Wang Z, Zhou L, Zou J, Cheng H, Lu Z. Ultrafine $NaTi_2(PO_4)_3$ nanoparticles encapsulated in N-CNFs as ultra-stable electrode for sodium storage. *Front Chem*. **2018**;*6*:270.
61. Dong J, Zhang G, Wang X, Zhang S, Deng C. Cross-linked $Na_2VTi(PO_4)_3$@C hierarchical nanofibers as high-performance bi-functional electrodes for symmetric aqueous rechargeable sodium batteries. *J Mater Chem A*. **2017**;*5*:18725.
62. Kim J, Seo D-H, Kim H, Park I, Yoo J-K, Jung S-K, Park Y-U, Goddard Iii WA, Kang K. Unexpected discovery of low-cost maricite $NaFePO_4$ as a high-performance electrode for Na-ion batteries. *Energy Environ Sci*. **2015**;*8*:540.
63. Liu Y, Zhang N, Wang F, Liu X, Jiao L, Fan L-Z. Approaching the downsizing limit of maricite $NaFePO_4$ toward high-performance cathode for sodium-ion batteries. *Adv Func Mater*. **2018**;*28*:1801917.
64. Barker J, Saidi MY, Swoyer JL. A sodium-ion cell based on the fluorophosphate compound $NaVPO_4F$. *Electrochem Solid-State Lett*. **2003**;*6*:A1.
65. Jin T, Liu Y, Li Y, Cao K, Wang X, Jiao L. Electrospun $NaVPO_4F$/C nanofibers as self-standing cathode material for ultralong cycle life na-ion batteries. *Adv Energy Mater*. **2017**;*7*:1700087.
66. Hu Y, Wu L, Liao G, Yang Y, Ye F, Chen J, Zhu X, Zhong S. Electrospinning synthesis of Na_2MnPO_4F/C nanofibers as a high voltage cathode material for Na-ion batteries. *Ceram Int*. **2018**;*44*:17577.
67. Wang F, Zhang N, Zhao X, Wang L, Zhang J, Wang T, Liu F, Liu Y, Fan LZ. Realizing a high-performance na-storage cathode by tailoring ultrasmall Na_2FePO_4F nanoparticles with facilitated reaction kinetics. *Adv Sci*. **2019**;*6*:1900649.
68. Niu Y, Xu M, Bao SJ, Li CM. Porous graphene to encapsulate $Na_{6.24}Fe_{4.88}(P_2O_7)_4$ as composite cathode materials for Na-ion batteries. *Chem Commun*. **2015**;*51*:13120.
69. Niu Y, Xu M, Dai C, Shen B, Li CM. Electrospun graphene-wrapped $Na_{6.24}Fe_{4.88}(P_2O_7)_4$ nanofibers as a high-performance cathode for sodium-ion batteries. *Phys Chem Chem Phys*. **2017**;*19*:17270.
70. Meng Y, Yu T, Zhang S, Deng C. Top-down synthesis of muscle-inspired alluaudite $Na_{2+2x}Fe_{2-x}(SO_4)_3$/SWNT spindle as a high-rate and high-potential cathode for sodium-ion batteries. *J Mater Chem A*. **2016**;*4*:1624.
71. Yu T, Lin B, Li Q, Wang X, Qu W, Zhang S, Deng C. First exploration of freestanding and flexible $Na_{2+2x}Fe_{2-x}(SO_4)_3$@porous carbon nanofiber hybrid films with superior sodium intercalation for sodium ion batteries. *Phys Chem Chem Phys*. **2016**;*18*:26933.
72. Luo W, Shen F, Bommier C, Zhu H, Ji X, Hu L. Na-ion battery anodes: materials and electrochemistry. *Acc Chem Res*. **2016**;*49*:231.
73. Ding J, Wang H, Li Z, Kohandehghan A, Cui K, Xu Z, Zahiri B, Tan X, Lotfabad EM, Olsen BC, Mitlin D. Carbon nanosheet frameworks derived from peat moss as high performance sodium ion battery anodes. *ACS Nano*. **2013**;*7*:11004.
74. Hou H, Banks CE, Jing M, Zhang Y, Ji X. Carbon quantum dots and their derivative 3D porous carbon frameworks for sodium-ion batteries with ultralong cycle life. *Adv Mater*. **2015**;*27*:7861.
75. Rybarczyk MK, Li Y, Qiao M, Hu Y-S, Titirici M-M, Lieder M. Hard carbon derived from rice husk as low cost negative electrodes in Na-ion batteries. *J Energy Chem*. **2019**;*29*:17.
76. Qiu D, Cao T, Zhang J, Zhang S-W, Zheng D, Wu H, Lv W, Kang F, Yang Q-H. Precise carbon structure control by salt template

for high performance sodium-ion storage. *J Energy Chem*. **2019**;*31*:101.
77. Xu Z-L, Liu X, Luo Y, Zhou L, Kim J-K. Nanosilicon anodes for high performance rechargeable batteries. *Prog Mater Sci*. **2017**;*90*:1.
78. Zhang B, Kang F, Tarascon J-M, Kim J-K. Recent advances in electrospun carbon nanofibers and their application in electrochemical energy storage. *Prog Mater Sci*. **2016**;*76*:319.
79. Bai Y, Wang Z, Wu C, Xu R, Wu F, Liu Y, Li H, Li Y, Lu J, Amine K. Hard carbon originated from polyvinyl chloride nanofibers as high-performance anode material for Na-ion battery. *ACS Appl Mater Interfaces*. **2015**;*7*:5598.
80. Chen T, Liu Y, Pan L, Lu T, Yao Y, Sun Z, Chua DHC, Chen Q. Electrospun carbon nanofibers as anode materials for sodium ion batteries with excellent cycle performance. *J Mater Chem A*. **2014**;*2*:4117.
81. Jin J, Shi Z-Q, Wang C-Y. Electrochemical performance of electrospun carbon nanofibers as free-standing and binder-free anodes for sodium-ion and lithium-ion batteries. *Electrochim Acta*. **2014**;*141*:302.
82. Guo X, Zhang X, Song H, Zhou J. Electrospun cross-linked carbon nanofiber films as free-standing and binder-free anodes with superior rate performance and long-term cycling stability for sodium ion storage. *J Mater Chem A*. **2017**;*5*:21343.
83. Maier J. Nanoionics: ion transport and electrochemical storage in confined systems. *Nat Mater*. **2005**;*4*:805.
84. Wang J, Li W, Yang Z, Gu L, Yu Y. Free-standing and binder-free sodium-ion electrodes based on carbon-nanotube decorated $Li_4Ti_5O_{12}$ nanoparticles embedded in carbon nanofibers. R Soc Chem Adv. 2014;4:25220.
85. Wang S, Xia L, Yu L, Zhang L, Wang H, Lou XW. Free-standing nitrogen-doped carbon nanofiber films: integrated electrodes for sodium-ion batteries with ultralong cycle life and superior rate capability. *Adv Energy Mater*. **2016**;*6*:1502217.
86. Dirican M, Zhang X. Centrifugally-spun carbon microfibers and porous carbon microfibers as anode materials for sodium-ion batteries. *J Power Sources*. **2016**;*327*:333.
87. Zeng L, Li W, Cheng J, Wang J, Liu X, Yu Y. N-doped porous hollow carbon nanofibers fabricated using electrospun polymer templates and their sodium storage properties. *R Soc Chem Adv*. **2014**;*4*:16920.
88. Zhu J, Chen C, Lu Y, Ge Y, Jiang H, Fu K, Zhang X. Nitrogen-doped carbon nanofibers derived from polyacrylonitrile for use as anode material in sodium-ion batteries. *Carbon*. **2015**;*94*:189.
89. Jin J, Yu B-J, Shi Z-Q, Wang C-Y, Chong C-B. Lignin-based electrospun carbon nanofibrous webs as free-standing and binder-free electrodes for sodium ion batteries. *J Power Sources*. **2014**;*272*:800.
90. Wu J, Yu J, Liu J, Cui J, Yao S, Ihsan-Ul Haq M, Mubarak N, Susca A, Ciucci F, Kim J-K. $MoSe_2$ nanosheets embedded in nitrogen/phosphorus co-doped carbon/graphene composite anodes for ultrafast sodium storage. *J Power Sources*. **2020**;*476*:228660.
91. Li Y, Chen M, Liu B, Zhang Y, Liang X, Xia X. Heteroatom doping: an effective way to boost sodium ion storage. *Adv Energy Mater*. **2020**;*10*:2000927.
92. Zou L, Lai Y, Hu H, Wang M, Zhang K, Zhang P, Fang J, Li J. N/S co-doped 3 D porous carbon nanosheet networks enhancing anode performance of sodium-ion batteries. *Chemistry*. **2017**;*23*:14261.
93. Zhang X, Zhu G, Wang M, Li J, Lu T, Pan L. Covalent-organic-frameworks derived N-doped porous carbon materials as anode for superior long-life cycling lithium and sodium ion batteries. *Carbon*. **2017**;*116*:686.
94. Yan D, Yu C, Zhang X, Qin W, Lu T, Hu B, Li H, Pan L. Nitrogen-doped carbon microspheres derived from oatmeal as high capacity and superior long life anode material for sodium ion battery. *Electrochim Acta*. **2016**;*191*:385.
95. Song H, Li N, Cui H, Wang C. Enhanced storage capability and kinetic processes by pores- and hetero-atoms-riched carbon nanobubbles for lithium-ion and sodium-ion batteries anodes. *Nano Energy*. **2014**;*4*:81.
96. Wang M, Yang Z, Li W, Gu L, Yu Y. Superior sodium storage in 3D interconnected nitrogen and oxygen dual-doped carbon network. *Small*. **2016**;*12*:2559.
97. Liu C, Hu J, Yang L, Zhao W, Li H, Pan F. Low-surface-area nitrogen doped carbon nanomaterials for advanced sodium ion batteries. *Chem Commun*. **2018**;*54*:2142.
98. Fu L, Tang K, Song K, van Aken PA, Yu Y, Maier J. Nitrogen doped porous carbon fibres as anode materials for sodium ion batteries with excellent rate performance. *Nanoscale*. **2014**;*6*:1384.
99. Liu Y, Zhang N, Yu C, Jiao L, Chen J. $MnFe_2O_4$@C nanofibers as high-performance anode for sodium-ion batteries. *Nano Lett*. **2016**;*16*:3321.
100. Chen C, Lu Y, Ge Y, Zhu J, Jiang H, Li Y, Hu Y, Zhang X. Synthesis of nitrogen-doped electrospun carbon nanofibers as anode material for high-performance sodium-ion batteries. *Energ Technol*. **2016**;*4*:1440.
101. Xu X, Zeng H, Han D, Qiao K, Xing W, Rood MJ, Yan Z. Nitrogen and sulfur co-doped graphene nanosheets to improve anode materials for sodium-ion batteries. ACS *Appl Mater Interfaces*. **2018**;*10*:37172.
102. Bao Y, Huang Y, Song X, Long J, Wang S, Ding L-X, Wang H. Heteroatom doping and activation of carbon nanofibers enabling ultrafast and stable sodium storage. *Electrochim Acta*. **2018**;*276*:304.
103. Sun X, Wang C, Gong Y, Gu L, Chen Q, Yu Y. A flexible sulfur-enriched nitrogen doped multichannel hollow carbon nanofibers film for high performance sodium storage. *Small*. **2018**;*14*:1802218.
104. Hou H, Shao L, Zhang Y, Zou G, Chen J, Ji X. Large-area carbon nanosheets doped with phosphorus: a high-performance anode material for sodium-ion batteries. *Adv Sci*. **2017**;*4*:1600243.
105. Li Y, Yuan Y, Bai Y, Liu Y, Wang Z, Li L, Wu F, Amine K, Wu C, Lu J. Insights into the Na^+ storage mechanism of phosphorus-functionalized hard carbon as ultrahigh capacity anodes. *Adv Energy Mater*. **2018**;*8*:1702781.
106. Wu F, Dong R, Bai Y, Li Y, Chen G, Wang Z, Wu C. Phosphorus-doped hard carbon nanofibers prepared by electrospinning as an anode in sodium-ion batteries. ACS *Appl Mater Interfaces*. **2018**;*10*:21335.
107. Zhu Y, Han X, Xu Y, Liu Y, Zheng S, Xu K, Hu L, Wang C. Electrospun Sb/C fibers for a stable and fast sodium-ion battery anode. *ACS Nano*. **2013**;*7*:6378.
108. Wu L, Hu X, Qian J, Pei F, Wu F, Mao R, Ai X, Yang H, Cao Y. Sb–C nanofibers with long cycle life as an anode material for high-performance sodium-ion batteries. *Energy Environ Sci*. **2014**;*7*:323.
109. Yin H, Li Q, Cao M, Zhang W, Zhao H, Li C, Huo K, Zhu M. Nanosized-bismuth-embedded 1D carbon nanofibers as high-performance anodes for lithium-ion and sodium-ion batteries. *Nano Res*. **2017**;*10*:2156.
110. Jin Y, Yuan H, Lan J-L, Yu Y, Lin Y-H, Yang X. Bio-inspired spider-web-like membranes with a hierarchical structure for high performance lithium/sodium ion battery electrodes: the case of 3D freestanding and binder-free bismuth/CNF anodes. *Nanoscale*. **2017**;*9*:13298.
111. Kim J-C, Kim D-W. Synthesis of multiphase SnSb nanoparticles-on-SnO_2/Sn/C nanofibers for use in Li and Na ion battery electrodes. *Electrochem Commun*. **2014**;*46*:124.

112. Jia H, Dirican M, Chen C, Zhu J, Zhu P, Yan C, Li Y, Dong X, Guo J, Zhang X. Reduced graphene oxide-incorporated SnSb@CNF composites as anodes for high-performance sodium-ion batteries. *ACS Appl Mater Interfaces*. **2018**;*10*:9696.
113. Kim J-C, Kim D-W. Electrospun Cu/Sn/C nanocomposite fiber anodes with superior usable lifetime for lithium- and sodium-ion batteries. *Chem Asian J*. **2014**;*9*:3313.
114. Mao M, Yan F, Cui C, Ma J, Zhang M, Wang T, Wang C. Pipe-wire TiO_2–Sn@carbon nanofibers paper anodes for lithium and sodium ion batteries. *Nano Lett*. **2017**;*17*:3830.
115. Ji L, Gu M, Shao Y, Li X, Engelhard MH, Arey BW, Wang W, Nie Z, Xiao J, Wang C, Zhang J-G, Liu J. Controlling SEI formation on SnSb-porous carbon nanofibers for improved Na ion storage. *Adv Mater*. **2014**;*26*:2901.
116. Chen C, Fu K, Lu Y, Zhu J, Xue L, Hu Y, Zhang X. Use of a tin antimony alloy-filled porous carbon nanofiber composite as an anode in sodium-ion batteries. *R Soc Chem Adv*. **2015**;*5*:30793.
117. Liu Y, Zhang N, Jiao L, Chen J. Tin nanodots encapsulated in porous nitrogen-doped carbon nanofibers as a free-standing anode for advanced sodium-ion batteries. *Adv Mater*. **2015**;*27*:6702.
118. Xu Z-L, Yao S, Cui J, Zhou L, Kim J-K. Atomic scale, amorphous FeO_x/carbon nanofiber anodes for Li-ion and Na-ion batteries. *Energy Storage Mater*. **2017**;*8*:10.
119. Xia G, Gao Q, Sun D, Yu X. Porous carbon nanofibers encapsulated with peapod-like hematite nanoparticles for high-rate and long-life battery anodes. *Small*. **2017**;*13*:1701561.
120. Yin H, Cao M-L, Yu X-X, Zhao H, Shen Y, Li C, Zhu M-Q. Self-standing Bi_2O_3 nanoparticles/carbon nanofiber hybrid films as a binder-free anode for flexible sodium-ion batteries. *Mater Chem Front*. **2017**;*1*:1615.
121. Wu L, Lang J, Wang R, Guo R, Yan X. Electrospinning synthesis of mesoporous $MnCoNiO_x$@double-carbon nanofibers for sodium-ion battery anodes with pseudocapacitive behavior and long cycle life. *ACS Appl Mater Interfaces*. **2016**;*8*:34342.
122. Zou W, Fan C, Li J. Sodium titanate/carbon ($Na_2Ti_3O_7$/C) nanofibers via electrospinning technique as the anode of sodium-ion batteries. *Chin J Chem*. **2017**;*35*:79.
123. Yang L, Zhu YE, Sheng J, Li F, Tang B, Zhang Y, Zhou Z. T-Nb_2O_5/C nanofibers prepared through electrospinning with prolonged cycle durability for high-rate sodium-ion batteries induced by pseudocapacitance. *Small*. **2017**;*13*:1702588.
124. Wang X, Liu Y, Wang Y, Jiao L. CuO quantum dots embedded in carbon nanofibers as binder-free anode for sodium ion batteries with enhanced properties. *Small*. **2016**;*12*:4865.
125. Liu Y, Wang F, Fan L-Z. Self-standing Na-storage anode of Fe_2O_3 nanodots encapsulated in porous N-doped carbon nanofibers with ultra-high cyclic stability. *Nano Res*. **2018**;*11*:4026.
126. Yao S, Cui J, Lu Z, Xu Z-L, Qin L, Huang J, Sadighi Z, Ciucci F, Kim J-K. Unveiling the unique phase transformation behavior and sodiation kinetics of 1D van der Waals Sb_2S_3 anodes for sodium ion batteries. *Adv Energy Mater*. **2017**;*7*:1602149.
127. Hayashi A, Masuzawa N, Yubuchi S, Tsuji F, Hotehama C, Sakuda A, Tatsumisago M. A sodium-ion sulfide solid electrolyte with unprecedented conductivity at room temperature. *Nat Commun*. **2019**;*10*:5266.
128. Wu J, Liu J, Cui J, Yao S, Ihsan-Ul-Haq M, Mubarak N, Quattrocchi E, Ciucci F, Kim J-K. Dual-phase MoS_2 as a high-performance sodium-ion battery anode. *J Mater Chem A*. **2020**;*8*:2114.
129. Wu J, Lu Z, Li K, Cui J, Yao S, Ihsan-ul Haq M, Li B, Yang Q-H, Kang F, Ciucci F, Kim J-K. Hierarchical MoS_2/carbon microspheres as long-life and high-rate anodes for sodium-ion batteries. *J Mater Chem A*. **2018**;*6*:5668.
130. Wu J, Ihsan-Ul-Haq M, Ciucci F, Huang B, Kim J-K. Rationally designed nanostructured metal chalcogenides for advanced sodium-ion batteries. *Energy Storage Mater*. **2021**;*34*:582.
131. Chen YM, Yu XY, Li Z, Paik U, Lou XW. Hierarchical MoS_2 tubular structures internally wired by carbon nanotubes as a highly stable anode material for lithium-ion batteries. *Sci Adv*. **2016**;*2*:1600021.
132. Chen C, Li G, Lu Y, Zhu J, Jiang M, Hu Y, Cao L, Zhang X. Chemical vapor deposited MoS_2/electrospun carbon nanofiber composite as anode material for high-performance sodium-ion batteries. *Electrochim Acta*. **2016**;*222*:1751.
133. Zhu C, Mu X, van Aken PA, Yu Y, Maier J. Single-layered ultrasmall nanoplates of MoS_2 embedded in carbon nanofibers with excellent electrochemical performance for lithium and sodium storage. *Angew Chem Int Ed*. **2014**;*53*:2152.
134. Cui C, Wei Z, Xu J, Zhang Y, Liu S, Liu H, Mao M, Wang S, Ma J, Dou S. Three-dimensional carbon frameworks enabling MoS_2 as anode for dual ion batteries with superior sodium storage properties. *Energy Storage Mater*. **2018**;*15*:22.
135. Jung J-W, Ryu W-H, Yu S, Kim C, Cho S-H, Kim I-D. Dimensional effects of MoS_2 nanoplates embedded in carbon nanofibers for bifunctional Li and Na insertion and conversion reactions. *ACS Appl Mater Interfaces*. **2016**;*8*:26758.
136. Zhao C, Yu C, Zhang M, Sun Q, Li S, Norouzi Banis M, Han X, Dong Q, Yang J, Wang G, Sun X, Qiu J. Enhanced sodium storage capability enabled by super wide-interlayer-spacing MoS_2 integrated on carbon fibers. *Nano Energy*. **2017**;*41*:66.
137. Ni Q, Bai Y, Guo S, Ren H, Chen G, Wang Z, Wu F, Wu C. Carbon nanofiber elastically confined nanoflowers: a highly efficient design for molybdenum disulfide-based flexible anodes toward fast sodium storage. *ACS Appl Mater Interfaces*. **2019**;*11*:5183.
138. Li W, Bi R, Liu G, Tian Y, Zhang L. 3D interconnected MoS_2 with enlarged interlayer spacing grown on carbon nanofibers as a flexible anode toward superior sodium-ion batteries. *ACS Appl Mater Interfaces*. **2018**;*10*:26982.
139. Xia J, Liu L, Jamil S, Xie J, Yan H, Yuan Y, Zhang Y, Nie S, Pan J, Wang X, Cao G. Free-standing SnS/C nanofiber anodes for ultralong cycle-life lithium-ion batteries and sodium-ion batteries. *Energy Storage Mater*. **2019**;*17*:1.
140. Chen Z, Chen S, Zhang H, Liu M, Feng Z, Li X, Huang J, Guo D. Exfoliated MoS_2@C nanosheets as anode for sodium/potassium storage. *Ionics*. **2019**;*26*:1779.
141. Liang J, Wei Z, Wang C, Ma J. Vacancy-induced sodium-ion storage in N-doped carbon Nanofiber@MoS_2 nanosheet arrays. *Electrochim Acta*. **2018**;*285*:301.
142. Cho E, Song K, Park MH, Nam K-W, Kang Y-M. SnS 3D flowers with superb kinetic properties for anodic use in next-generation sodium rechargeable batteries. *Small*. **2016**;*12*:2510.
143. Zhang S, Zhao H, Wang M, Li Z, Mi J. Low crystallinity SnS encapsulated in CNTs decorated and S-doped carbon nanofibers as excellent anode material for sodium-ion batteries. *Electrochim Acta*. **2018**;*279*:186.
144. Wang Y, Zhang Y, Shi J, Kong X, Cao X, Liang S, Cao G, Pan A. Tin sulfide nanoparticles embedded in sulfur and nitrogen dual-doped mesoporous carbon fibers as high-performance anodes with battery-capacitive sodium storage. *Energy Storage Mater*. **2019**;*18*:366.
145. Xia J, Jiang K, Xie J, Guo S, Liu L, Zhang Y, Nie S, Yuan Y, Yan H, Wang X. Tin disulfide embedded in N-, S-doped carbon nanofibers as anode material for sodium-ion batteries. *Chem Eng J*. **2019**;*359*:1244.
146. Gao B, Li X, Ding K, Huang C, Li Q, Chu PK, Huo K. Recent progress in nanostructured transition metal nitrides for advanced electrochemical energy storage. *J Mater Chem A*. **2019**;*7*:14.
147. Luo Y, Huang D, Liang C, Wang P, Han K, Wu B, Cao F, Mai L, Chen H. Fe_2VO_4 hierarchical porous microparticles prepared via a facile surface solvation treatment for high-performance lithium and sodium storage. *Small*. **2019**;*15*:1804706.

148. Xu L, Xiong P, Zeng L, Fang Y, Liu R, Liu J, Luo F, Chen Q, Wei M, Qian Q. Electrospun $VSe_{1.5}$/CNF composite with excellent performance for alkali metal ion batteries. *Nanoscale*. **2019**;*11*:16308.
149. Xu L, Xiong P, Zeng L, Liu R, Liu J, Luo F, Li X, Chen Q, Wei M, Qian Q. Facile fabrication of a vanadium nitride/carbon fiber composite for half/full sodium-ion and potassium-ion batteries with long-term cycling performance. *Nanoscale*. **2020**;*12*:10693.

Chuanping Li received his BS degree from Jiaying University in 2020. Currently, he is a MS student under the supervision of Prof. Yuming Chen at Fujian Normal University. His research interests focus on sodium-ion batteries, engineering of carbon nanomaterials and their applications.

Min Qiu is pursuing her master degree in College of Chemistry and Materials Sciences at Fujian Normal University. Her research focuses on computational chemistry.

Ruiling Li received a bachelor's degree from Shanxi Normal University in 2020. Now she is a master student under the guidance of Professor Xiaoyan Li of Fujian Normal University. Her research interests focus on sodium-ion batteries, metal sulfide anode materials and their applications.

Xuan Li is studying a master degree in resource recycling science and engineering from Fujian Normal University under Prof. Qinghua Chen and Prof. Yuming Chen. His research focuses on nanostructured carbon materials for sodium/potassium-ion batteries.

Manxi Wang is now studying her doctoral degree in Environmental Chemistry at Fujian Normal University under Prof. Qinghua Chen and Prof. Yuming Chen. Her research interests focus on solid-sate lithium metal batteries and lithium ion batteries.

Jiabo He is pursuing his master degree at Fujian Normal University under the supervision of Prof. Xiaoyan Li. His research focuses on computational chemistry.

Ganggang Lin is an Electrical Engineer work in State Grid Fujian Electric Power Maintenance Company. He received a M.Sc. in Electrical Engineering Automation at Fuzhou University. He has been engaged in power transformation, operation and maintenance for 13 years. His research interests focus on the UHV power transmission and transformation.

Liren Xiao is a full Professor of College of Chemistry and Materials Sciences at Fujian Normal University. She has co-authored over 100 papers and 20 invention patents. Her researches mainly focus on environmental materials and solid waste comprehensive utilization.

Qingrong Qian is the dean of the College of Environmental Science and Engineering at Fujian Normal University. He completed his postdoctoral research at the University of Tokyo, and he has co-authored more than 200 papers and 23 patents. His researches mainly focus on environmental materials and solid waste comprehensive utilization.

Qinghua Chen is the director of Engineering Research Center of Polymer Green Recycling of Ministry of Education and the vice-president of Fujian Normal University. He has co-authored ~400 papers and ~30 invention patents. His group mainly focuses on environmental materials and solid waste comprehensive utilization.

Junxiong Wu received his B. S. from Fuzhou University and M.E. from Tsinghua University in 2013 and 2016, respectively. He earned his Ph.D. in Mechanical Engineering from The Hong Kong University of Science and Technology in 2020. Currently, he is a Postdoctoral Fellow at The Hong Kong Polytechnic University. His research focuses on new materials and advanced characterization for Li/Na-ion batteries and alkali metal anodes.

Xiaoyan Li received her Ph.D. in 2015 from The Hong Kong Polytechnic University under Prof. Limin Zhou, Prof. Yiu-Wing Mai and Prof. Haitao Huang. During her PhD program, she worked with Prof. Xiaodong Chen in Nanyang Technological University as a visiting student. She received the Award Program for Minjiang Scholar Professorship. Her research interests mainly focus on electrospinning, environment-friendly materials, and energy storage.

Yiu-Wing Mai is University Professor in Mechanical Engineering at the University of Sydney. He obtained his PhD on fracture mechanics from the University of Hong Kong and pursued postdoctoral research at the University of Michigan and Imperial College London. His current interest is on multifunctional polymer nanocomposites. He is a fellow of the Royal Society and a foreign member of the Chinese Academy of Engineering.

Yuming Chen received his Ph.D. in 2014 from The Hong Kong Polytechnic University under Prof. Yiu-Wing Mai and Prof. Limin Zhou. During his PhD program, he worked with Prof. John B Goodenough in The University of Texas at Austin in 2013 as a visiting student. After his graduation, he became a postdoctoral researcher at NTU and MIT. His research interests include electrospinning, in situ TEM, and energy storage. He has published over 50 scientific papers in Nature, Chem, Sci. Adv., etc.